Neutrinoless double-β decay in the microscopic interacting boson model

J. Barea and F. Iachello

Center for Theoretical Physics, Sloane Physics Laboratory, Yale University, New Haven, Connecticut 06520-8120, USA

(Received 6 November 2008; revised manuscript received 3 February 2009; published 2 April 2009)

We present a formalism for calculating nuclear matrix elements of double-β decay within the framework of the microscopic interacting boson model. We calculate Fermi, Gamow-Teller, and tensor matrix elements in the decay of Ge-Se-Mo-Te-Xe-Nd-Sm and compare our results with those of the shell-model (SM) and of the quasiparticle random-phase approximation (QRPA). Our results are in agreement with QRPA. We discuss simple features of the matrix elements and give a formula that allows one to estimate matrix elements in terms of the number of valence proton and neutron pairs.

DOI: 10.1103/PhysRevC.79.044301 PACS number(s): 23.40.Hc, 21.60.Fw, 27.50.+e, 27.60.+j

I. INTRODUCTION

Recent experiments [1–3] appear to indicate that neutrinos have a nonzero mass, $m_\nu \neq 0$. A direct measurement of the average neutrino mass (if the neutrino is a Majorana particle) can be obtained from the observation of the neutrinoless double-β decay

$$ {}^A_Z X_N \rightarrow {}^A_{Z+2} Y_{N-2} + 2e^-. \tag{1}$$

Apart from an unconfirmed experiment [4], this process has not yet been observed, but several experiments are underway [5,6] and others are in the planning stage. It is therefore of importance to provide estimates of the expected lifetime for the decay. The half-life of $0\nu\beta\beta$ decay can be written as

$$ \left[T^{0\nu\beta\beta}_{1/2}(0^+ \rightarrow 0^+)\right]^{-1} = G_{0\nu} |M^{(0\nu)}|^2 \left(\frac{\langle m_\nu \rangle}{m_e}\right)^2, \tag{2}$$

where $\langle m_\nu \rangle = \sum_k |U_{\nu k}|^2 m_k$ is the average neutrino mass, $G_{0\nu}$ is a kinematic factor dependent on the charge, mass and available energy, and $M^{(0\nu)}$ is the nuclear matrix element. A crucial ingredient in the evaluation of the lifetime is the nuclear matrix element. This matrix element depends on the form of the hadronic current, J^μ_L, which appears in the weak Hamiltonian and on the structure of the initial and final nuclei. Given a model for the origin of the neutrino mass, one can write down the associated hadronic current. On reduction to its nonrelativistic form, one can write a transition operator V and evaluate its matrix elements between initial and final states. This evaluation is in general rather difficult, because, in the decay from an even-even nucleus, $N =$ even, $Z =$ even, to another even-even nucleus one needs to know the structure of the intermediate odd-odd nucleus. However, for neutrinoless double-β decay the average neutrino momentum is of the order of 100 MeV and one can therefore use the *closure* approximation. (The closure approximation may not be good for double-β decay with emission of two neutrinos where the average momentum is small.) Using the closure approximation, the calculation of the nuclear matrix elements amounts to the calculation of a two-body matrix element. Three types of matrix elements play a particularly important role, Fermi (F), Gamow-Teller (GT), and tensor (T) matrix elements.

Two methods have been used so far to evaluate the nuclear matrix elements, the shell model (SM) in its original version [7] and in very recent large scale versions [8], and the quasiparticle random-phase approximation (QRPA) in its early form [9] and in its more recent versions [10]. In this article, we propose a third method, the microscopic interacting boson model (IBM). Our purpose is threefold: (i) to provide an independent calculation and investigate the sensitivity of the results to assumptions made concerning the single-particle energies and strengths of interactions; (ii) to make use of wave functions of initial and final nuclei which are as much as possible *realistic*, i.e., that describe accurately the known properties of those nuclei; and (iii) to extract simple features, if any, of the otherwise complex calculation.

The article is structured as follows. In Secs. II–IV, we derive the formalism needed to evaluate the matrix elements of Fermi, Gamow-Teller, and tensor interactions in the microscopic interacting boson model. This proceeds by evaluating the fermionic two-body matrix elements $G(j_1, j_2, j_1', j_2'; J)$ and thus writing the general second-quantized fermionic transition operator (Sec. II). The matrix elements of this operator are then evaluated in the generalized seniority scheme in Sec. III. Finally, this operator is mapped into a bosonic second-quantized transition operator (Sec. IV) and its matrix elements are evaluated using realistic IBM-2 wave functions. In Sec. V we show our results and compare with the results of the SM and the QRPA. In Sec. VI we discuss some simple features of the calculation and present a simple formula that allows one to estimate the matrix elements in terms of the number of proton and neutron valence pairs.

II. FERMIONIC TRANSITION OPERATORS

We are interested in the matrix elements of the F, GT, and T operators. The fermionic transition operator for F, GT, and T can be written compactly as

$$ V^{(\lambda)}_{s_1,s_2} = \frac{1}{2} \sum_{n,n'} \tau^+_n \tau^+_{n'} \left[\Sigma^{(s_1)}_n \times \Sigma^{(s_2)}_{n'}\right]^{(\lambda)} \cdot V(r_{nn'}) C^{(\lambda)}(\Omega_{nn'}), \tag{3}$$

where, for $s = 0$, $\Sigma^{(0)} = 1$, and, for $s = 1$, $\Sigma^{(1)} = \vec{\sigma}$. $V(r)$ is a generic radial form that depends on the model of double-β decay and $C^{(\lambda)} = \sqrt{4\pi/(2\lambda+1)}Y^{(\lambda)}$ (we use the notation of de-Shalit and Talmi [11]). In this compact form, the Fermi term has $\lambda = 0$, $s_1 = s_2 = 0$, the Gamow-Teller term has $\lambda = 0$, $s_1 = s_2 = 1$, with an additional factor of $(-1)^{s_1}\sqrt{2s_1+1} = -\sqrt{3}$, and the tensor term has $\lambda = 2$, $s_1 = s_2 = 1$, with an additional factor of $\sqrt{\frac{2}{3}}$.

Introducing creation and annihilation operators for single particle states, $c^\dagger_{nljm}$, the two-particle states can be written as

$$|(n_1 l_1 j_1)(n_2 l_2 j_2); JM\rangle = \frac{\left(c^\dagger_{n_1 l_1 j_1} \times c^\dagger_{n_2 l_2 j_2}\right)^{(J)}_M |0\rangle}{\sqrt{1+(-1)^J \delta_{n_1 n_2}\delta_{l_1 l_2}\delta_{j_1 j_2}}}, \quad (4)$$

and the second-quantized fermion operator as

$$\begin{aligned} V^{(\lambda)}_{s_1,s_2} = &-\frac{1}{4}\sum_{j_1 j_2}\sum_{j_1' j_2'}\sum_J (-1)^J \sqrt{1+(-1)^J\delta_{j_1 j_2}} \\ &\times \sqrt{1+(-1)^J\delta_{j_1' j_2'}}\, G^{(\lambda)}_{s_1 s_2}(j_1 j_2 j_1' j_2'; J) \\ &\times \left(\pi^\dagger_{j_1} \times \pi^\dagger_{j_2}\right)^{(J)} \cdot \left(\tilde{\nu}_{j_1'} \times \tilde{\nu}_{j_2'}\right)^{(J)}, \end{aligned} \quad (5)$$

where $\hat{J} = \sqrt{2J+1}$ and $\pi^\dagger_{nljm}(\tilde{\nu}_{nljm})$ creates (destroys) a proton (neutron) in the single-particle state $|nljm\rangle$. $G^{(\lambda)}_{s_1 s_2}(j_1 j_2 j_1' j_2'; J)$ is the two-body matrix element of $V^{(\lambda)}_{s_1 s_2}$ between two-fermion states

$$\begin{aligned} G^{(\lambda)}_{s_1 s_2}(j_1 j_2 j_1' j_2'; J) = &\sum_{k_1=|l_1-l_1'|}^{l_1+l_1'} \sum_{k_2=|l_2-l_2'|}^{l_2+l_2'} \sum_{k=k_{\min}}^{k_{\max}} i^{k_1-k_2+\lambda}\hat{k}_1^2\hat{k}_2^2 \\ &\times \langle k_1 0 k_2 0|\lambda 0\rangle (-1)^{s_2+k_1} \begin{Bmatrix} k_1 & s_1 & k \\ s_2 & k_2 & \lambda \end{Bmatrix} \\ &\times (-1)^{j_2+j_1'+J} \begin{Bmatrix} j_1 & j_2 & J \\ j_2' & j_1' & k \end{Bmatrix} \\ &\times \hat{k}\hat{j}_1\hat{j}_1' \begin{Bmatrix} \frac{1}{2} & l_1 & j_1 \\ \frac{1}{2} & l_1' & j_1' \\ s_1 & k_1 & k \end{Bmatrix} \hat{k}\hat{j}_2\hat{j}_2' \begin{Bmatrix} \frac{1}{2} & l_2 & j_2 \\ \frac{1}{2} & l_2' & j_2' \\ s_2 & k_2 & k \end{Bmatrix} \\ &\times \left\langle \frac{1}{2}\|\Sigma^{(s_1)}\|\frac{1}{2}\right\rangle (-1)^{-k_1}\hat{l}_1 \langle l_1 0 k_1 0|l_1' 0\rangle \\ &\times \left\langle \frac{1}{2}\|\Sigma^{(s_2)}\|\frac{1}{2}\right\rangle (-1)^{-k_2}\hat{l}_2 \left\langle l_2 0 k_2 0 \mid l_2' 0\right\rangle \\ &\times R^{(k_1,k_2,\lambda)}(n_1, l_1, n_2, l_2, n_1', l_1', n_2', l_2'), \end{aligned} \quad (6)$$

with $\langle \frac{1}{2}\|\Sigma^{(s)}\|\frac{1}{2}\rangle = \sqrt{2(2s+1)}$, $k_{\min} = \max(|j_1 - j_1'|, |j_2 - j_2'|)$, and $k_{\max} = \min(j_1 + j_1', j_2 + j_2')$. $R^{(k_1,k_2,\lambda)}(n_1 l_1, n_2, l_2; n_1' l_1', n_2' l_2')$ are the radial integrals and Appendix A describes how to calculate them.

III. MATRIX ELEMENTS IN THE GENERALIZED SENIORITY SCHEME

We consider matrix elements of the fermionic operators in the collective SD subspace formed by pair states with $J^P = 0^+$ and $J^P = 2^+$ of identical nucleons. The pair operators that create these states are written as

$$S^\dagger = \sum_j \alpha_j \sqrt{\frac{\Omega_j}{2}}(c^\dagger_j \times c^\dagger_j)^{(0)} \quad (7)$$

$$D^\dagger = \sum_{j \leqslant j'} \beta_{jj'} \frac{1}{\sqrt{1+\delta_{jj'}}}(c^\dagger_j \times c^\dagger_{j'})^{(2)} \quad (8)$$

with $\Omega_j = j + \frac{1}{2}$. Several methods have been used to determine the structure coefficients α_j and $\beta_{jj'}$. In this article we use the method of Ref. [12] with structure coefficients obtained by diagonalizing the surface delta interaction (SDI). Details are given in Appendix B. The SM states in the SD subspace are constructed as

$$|n, v, J\rangle = \eta^{-1}_{nvJ}(S^\dagger)^{\frac{n-v}{2}}|v, v, J\rangle, \quad (9)$$

where all labels other than seniority v and total angular momentum J have been omitted. η_{nvJ} is a normalization constant given in Appendix B. The states $|v, v, J\rangle$ represent states of maximum generalized seniority constructed with D pairs operators. For example, the state $|n = 2, v = 2, J = 2\rangle$ is given by

$$|n = 2, v = 2, J = 2\rangle = D^\dagger|0\rangle. \quad (10)$$

These states are properly normalized as long as the structure coefficients satisfy

$$\sum_{j \leqslant j'} \beta^2_{jj'} = 1. \quad (11)$$

The construction for higher seniorities is more complicated and is reported in Ref. [12].

Matrix elements of the fermion operator (5) can now be calculated. This requires the calculation of the matrix elements of the operators $(c^\dagger_j \times c^\dagger_{j'})^{(L)}$. We have used the commutator method developed by Frank and Van Isacker [13] and the work of Lipas *et al.* [14] to evaluate the matrix elements of these operators. Our (novel) results are shown in Appendix C. These general results are needed for the calculation of matrix elements in the interacting boson model, discussed in the following sections. In the "generalized seniority scheme" (GS), in which the wave functions of ground state of nuclei have $v = 0$, the double-β decay matrix elements depend only on the structure coefficients, α_j's. The corresponding matrix elements are denoted by GS in the table of results.

IV. MATRIX ELEMENTS IN THE INTERACTING BOSON MODEL

In the microscopic IBM [15], the shell-model SD pair states are mapped onto sd boson states with $J^P = 0^+$ and $J^P = 2^+$

$$S^\dagger \longmapsto s^\dagger \quad (12)$$

$$D^\dagger \longmapsto d^\dagger. \quad (13)$$

Fermionic operators are similarly mapped into bosonic operators by the Otsuka, Arima, and Iachello (OAI) method [16]. Using this method one is assured that the matrix elements between fermionic states in the collective subspace

are identical to the matrix elements in the bosonic space. In this article we first consider the simple mapping

$$(\pi_j^\dagger \times \pi_j^\dagger)^{(0)} \longmapsto A_\pi(j) s_\pi^\dagger \tag{14}$$

$$(\pi_j^\dagger \times \pi_{j'}^\dagger)^{(2)}_M \longmapsto B_\pi(j, j') d^\dagger_{\pi,M} \tag{15}$$

for protons and similar expression for neutrons. Using Eqs. (14) and (15) we obtain the bosonic image of the fermion operator of Eq. (5)

$$\begin{aligned} V^{(\lambda)}_{s_1 s_2} \longmapsto & -\frac{1}{2}\sum_{j_1}\sum_{j_1'} G^{(\lambda)}_{s_1 s_2}(j_1 j_1 j_1' j_1'; 0) \\ & \times A_\pi(j_1) A_\nu(j_1') s_\pi^\dagger \cdot \tilde{s}_\nu \\ & -\frac{1}{4}\sum_{j_1 j_2}\sum_{j_1' j_2'} \sqrt{1+\delta_{j_1 j_2}}\sqrt{1+\delta_{j_1' j_2'}} \\ & \times G^{(\lambda)}_{s_1 s_2}(j_1 j_2 j_1' j_2'; 2) B_\pi(j_1, j_2) B_\nu(j_1', j_2') d_\pi^\dagger \cdot \tilde{d}_\nu. \end{aligned} \tag{16}$$

The coefficients $A_\rho(j_1)$ and $B_\rho(j_1, j_2)\,(\rho = \nu, \pi)$ are given in Appendix D. [Because in the IBM particles (p) are considered in the first half of a major shell, and holes (h) in the second half, the mapping must respect particle-hole conjugation, i.e., $\tilde{s}_\nu, \tilde{d}_\nu$ must be replaced, in the second part of the shell, by $s_{\bar{\nu}}^\dagger, d_{\bar{\nu}}^\dagger$, where a bar denotes the conjugate state.]

A realistic set of wave functions of even-even nuclei with mass $A \gtrsim 60$ is provided by the proton-neutron IBM-2 [17]. The wave functions are generated by diagonalizing the IBM-2 Hamiltonian. The parameters of the complete set of nuclei in this calculation are given in Appendix E. The associated wave functions produce spectra and intensities of electromagnetic transitions in good agreement with experiment. Using these realistic wave functions and the operators of (16) we can calculate the matrix elements of double-β decay, denoted by IBM-2 in the tables of results.

The bosonization method, when carried to all orders, produces results that are identical to the fermionic results. To investigate the extent to which our calculations are reliable, we have carried out the OAI expansion to next to leading order (NLO)

$$\begin{aligned} (\pi_j^\dagger \times \pi_{j'}^\dagger)^{(2)}_M \longmapsto & B_\pi(j, j')(d_\pi^\dagger)_M + C_\pi(j, j') s_\pi^\dagger (s_\pi^\dagger \tilde{d}_\pi)^{(2)}_M \\ & + D_\pi(j, j') s_\pi^\dagger (d_\pi^\dagger \tilde{d}_\pi)^{(2)}_M. \end{aligned} \tag{17}$$

To this order, the bosonic operator becomes

$$\begin{aligned} V^{(\lambda)}_{s_1 s_2} \longmapsto & -\frac{1}{2}\sum_{j_1}\sum_{j_1'} G^{(\lambda)}_{s_1 s_2}(j_1 j_1 j_1' j_1'; 0) \\ & \times A_\pi(j_1) A_\nu(j_1') s_\pi^\dagger \cdot \tilde{s}_\nu \\ & -\frac{1}{4}\sum_{j_1 j_2}\sum_{j_1' j_2'} \sqrt{1+\delta_{j_1 j_2}}\sqrt{1+\delta_{j_1' j_2'}} \\ & \times G^{(\lambda)}_{s_1 s_2}(j_1 j_2 j_1' j_2'; 2) \\ & \times \{ B_\pi(j_1, j_2) B_\nu(j_1', j_2') d_\pi^\dagger \cdot \tilde{d}_\nu \\ & + B_\pi(j_1, j_2) C_\nu(j_1', j_2') d_\pi^\dagger \cdot \tilde{s}_\nu \tilde{s}_\nu d_\nu^\dagger \\ & + C_\pi(j_1, j_2) B_\nu(j_1', j_2') s_\pi^\dagger s_\pi^\dagger \tilde{d}_\pi \cdot \tilde{d}_\nu \\ & + C_\pi(j_1, j_2) C_\nu(j_1', j_2') s_\pi^\dagger s_\pi^\dagger \tilde{d}_\pi \cdot \tilde{s}_\nu \tilde{s}_\nu d_\nu^\dagger \\ & + B_\pi(j_1, j_2) D_\nu(j_1', j_2') d_\pi^\dagger \cdot \tilde{s}_\nu (d_\nu^\dagger \tilde{d}_\nu)^{(2)} \\ & + D_\pi(j_1, j_2) B_\nu(j_1', j_2') s_\pi^\dagger (d_\pi^\dagger \tilde{d}_\pi)^{(2)} \cdot \tilde{d}_\nu \\ & + C_\pi(j_1, j_2) D_\nu(j_1', j_2') s_\pi^\dagger s_\pi^\dagger \tilde{d}_\pi \cdot \tilde{s}_\nu (d_\nu^\dagger \tilde{d}_\nu)^{(2)} \\ & + D_\pi(j_1, j_2) C_\nu(j_1', j_2') s_\pi^\dagger (d_\pi^\dagger \tilde{d}_\pi)^{(2)} \cdot \tilde{s}_\nu \tilde{s}_\nu d_\nu^\dagger \\ & + D_\pi(j_1, j_2) D_\nu(j_1', j_2') s_\pi^\dagger (d_\pi^\dagger \tilde{d}_\pi)^{(2)} \cdot \tilde{s}_\nu (d_\nu^\dagger \tilde{d}_\nu)^{(2)} \}. \end{aligned} \tag{18}$$

with the (novel) coefficients $C_\rho(j_1, j_2)$ and $D_\rho(j_1, j_2)$ given in Appendix D. (A boson expansion of the pair operators up to the second term in Eq. (17) was carried out many years ago [18] for the purpose of calculating 2ν double-β decay matrix elements in the closure approximation.) Using Eq. (18) and the realistic wave functions we can compute the matrix elements denoted by IBM-2 NLO in the tables of results.

V. RESULTS

We divide the discussion of our results in two parts. In the first part, we study how our results depend on the approximations GS, IBM-2, and IBM-2 NLO. For this part we use the formulation of matrix elements of neutrinoless double-β decay of Tomoda *et al.* [9]. This formulation contains both terms proportional to the neutrino mass squared and terms proportional to other parameters $\langle\lambda\rangle$ and $\langle\eta\rangle$ of the decay model and is thus "complete." Our conclusion is that the effect of NLO boson terms is small for all (proportional and nonproportional to the neutrino mass squared) matrix elements.

In the second part, having established the smallness of the NLO terms for all matrix elements, we use IBM-2 to calculate neutrinoless double-β decay matrix elements in the more recent formulation of Šimkovic *et al.* [10]. This formulation is similar to that of Tomoda for F and GT matrix elements but with additional higher-order contributions, denoted by HOC. In particular, it has an induced tensor term that differs from Tomoda's both in radial dependence and in magnitude. Because this formulation is that used in very recent SM and QRPA calculations, we will use it in all further discussions and comparisons with other calculations.

A. Comparisons between GS, IBM-2, and IBM-2 NLO

To assess the role of approximations in the boson calculation, we use the formulation of matrix elements of neutrinoless double-β decay of Ref. [9]. In this formulation, two matrix elements appear in front of the neutrino mass squared $(\langle m_\nu\rangle/m_e)^2$, the Fermi, $M_F^{(0\nu)}$, and Gamow-Teller, $M_{\rm GT}^{(0\nu)}$, matrix elements

$$M_{\rm GT}^{(0\nu)} = \langle H(r_{12}) \vec{\sigma}_1 \cdot \vec{\sigma}_2 \rangle \tag{19}$$

$$\begin{aligned} \chi_F &= \left[M_{\rm GT}^{(0\nu)}\right]^{-1} (g_V/g_A)^2 \langle H(r_{12})\rangle \\ &= \left[M_{\rm GT}^{(0\nu)}\right]^{-1} (g_V/g_A)^2 M_F^{(0\nu)} \end{aligned} \tag{20}$$

the total matrix element being

$$M^{(0\nu)} = (-\chi_F + 1) M_{\rm GT}^{(0\nu)} = -(g_V/g_A)^2\, M_F^{(0\nu)} + M_{\rm GT}^{(0\nu)}, \tag{21}$$

with

$$M_F^{(0\nu)} = \langle H(r_{12}) \rangle \,. \tag{22}$$

In Tomoda's formulation, the bracket $\langle O_{12} \rangle$ is defined as

$$\langle O_{12} \rangle \equiv \frac{1}{2} \langle 0_F^+ | \sum_{n,n'} \tau_n^+ \tau_{n'}^+ O_{nn'} | 0_I^+ \rangle, \tag{23}$$

where $|0_{I,F}^+\rangle$ are the wave functions of the initial and final states and the potential $H(r_{12})$ is conveniently defined in momentum space, see Appendix A,

$$v(p) = \frac{2}{\pi} \frac{1}{p(p + \tilde{A})}, \tag{24}$$

where $\tilde{A}$ (the closure energy) is assumed to be a smoothly varying function of the mass number A given in Table 25 of Ref. [9]. Two corrections are usually included in the calculation of the matrix elements, the finite nucleon size (FNS) and the short range correlations (SRC). The finite nucleon size is taken into account in momentum space by replacing the coupling constants g_V, g_A by the dipole forms

$$g_V(p^2) = g_V \frac{1}{\left(1 + \frac{p^2}{M_V^2}\right)^2} \tag{25}$$

$$g_A(p^2) = g_A \frac{1}{\left(1 + \frac{p^2}{M_A^2}\right)^2}. \tag{26}$$

The value of $M_V^2 = 0.71$ $(\mathrm{GeV}/c^2)^2$ is well fixed by the electromagnetic form factor of the proton, while the value of $M_A = 1.09\ \mathrm{GeV}/c^2$ is estimated. The short-range correlations are usually taken into account by multiplying the potential $H(r)$ by the Jastrow function squared, $f(r)^2$, with

$$f(r) = 1 - e^{-ar^2}(1 - br^2), \tag{27}$$

where $a = 1.1\ \mathrm{fm}^{-2}$ and $b = 0.68\ \mathrm{fm}^{-2}$. The results of our calculation with the "experimental" set of parameters, Set I of Appendix B, are shown in Table I columns GS, IBM-2, and IBM-2 NLO. In this table, we also quote, for reference, the SM results in a restricted basis by Haxton [7] (from Table 7 of Ref. [9]) and the QRPA by Tomoda (from Table 17 of Ref. [9]) with $g_V = 1$, $g_A = 1.25$. There is an overall phase ambiguity in the definition of the matrix elements that is irrelevant when calculating the lifetime. We choose in this article, for the sake of comparison to other calculations, the phase convention of Tomoda [9]. Our calculations are in good agreement with both the SM and QRPA when protons and neutrons occupy the same major shell (Ge-Se-Te-Xe) but only in fair agreement when protons and neutrons occupy different major shells (Mo-Nd-Sm). For ^{136}Xe we have only done a generalized seniority calculation because this nucleus is semimagic ($N = 82$) and is well described by GS. When comparing our calculations GS, IBM-2, and IBM-2 NLO we observe that there is a systematic reduction of the matrix elements by about 20% when going from GS to IBM-2 while the effect of NLO terms is very small. This is shown for ^{76}Ge in Fig. 1, where the various contributions with their signs are plotted. This figure is reminiscent of Fig. 1 of Ref. [8]. We find that the contribution of s bosons is dominant, the contribution of d bosons is sizable and of opposite sign, whereas NLO

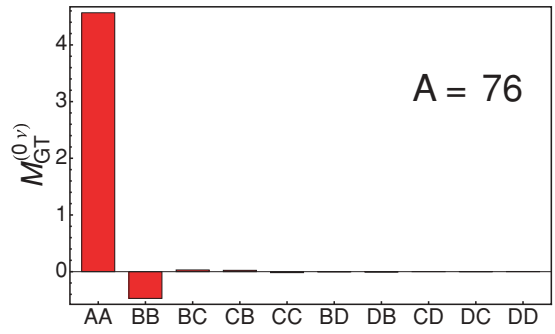

FIG. 1. (Color online) Contributions to the Gamow-Teller matrix elements of the ^{76}Ge $\rightarrow$ ^{76}Se decay in the boson expansion of Eq. (18).

corrections are small and with random sign. This result applies to all calculated nuclei.

In addition to terms proportional to $(\langle m_\nu \rangle / m_e)^2$, Tomoda considered also terms proportional to parameters $\langle \lambda \rangle$ and $\langle \eta \rangle$, where λ and η depend on the decay model and are defined on p. 75 of Ref. [9], nine terms in all: three Gamow-Teller (GT), three Fermi (F), one tensor (T), one pseudoscalar (P), and one recoil (R). We have calculated the first seven of those, the two discussed previously, $M_{\mathrm{GT}}^{(0\nu)}$, χ_F, and the five additional terms, $\tilde{\chi}_{\mathrm{GT}}$, $\tilde{\chi}_F$, χ'_{GT}, χ'_F, χ'_T,

$$M_{\mathrm{GT}}^{(0\nu)} = \langle H(r_{12}) \vec{\sigma}_1 \cdot \vec{\sigma}_2 \rangle \tag{28}$$

$$\chi_F = \left[M_{\mathrm{GT}}^{(0\nu)}\right]^{-1} (g_V/g_A)^2 \langle H(r_{12}) \rangle \tag{29}$$

$$\tilde{\chi}_{\mathrm{GT}} = \left[M_{\mathrm{GT}}^{(0\nu)}\right]^{-1} \langle \tilde{H}(r_{12}) \vec{\sigma}_1 \cdot \vec{\sigma}_2 \rangle \tag{30}$$

$$\tilde{\chi}_F = \left[M_{\mathrm{GT}}^{(0\nu)}\right]^{-1} (g_V/g_A)^2 \langle \tilde{H}(r_{12}) \rangle \tag{31}$$

$$\chi'_{\mathrm{GT}} = \left[M_{\mathrm{GT}}^{(0\nu)}\right]^{-1} \langle -r_{12} H'(r_{12}) \vec{\sigma}_1 \cdot \vec{\sigma}_2 \rangle \tag{32}$$

$$\chi'_F = \left[M_{\mathrm{GT}}^{(0\nu)}\right]^{-1} (g_V/g_A)^2 \langle -r_{12} H'(r_{12}) \rangle \tag{33}$$

$$\chi'_T = \left[M_{\mathrm{GT}}^{(0\nu)}\right]^{-1} \Big\langle -r_{12} H'(r_{12}) \Big[(\vec{\sigma}_1 \cdot \hat{r}_{12})(\vec{\sigma}_2 \cdot \hat{r}_{12}) - \tfrac{1}{3} \vec{\sigma}_1 \cdot \vec{\sigma}_2 \Big] \Big\rangle, \tag{34}$$

expressed as ratios to $M_{\mathrm{GT}}^{(0\nu)}$. Partial results are given in Table II where IBM-2 calculations are compared with those of Haxton and Tomoda, taken from the same sources as those of Table I. We omitted $\tilde{\chi}_{F,\mathrm{GT}}$ because they are related to $\chi'_{F,\mathrm{GT}}$ and χ_F by $\tilde{\chi}_{\mathrm{GT}} = 2 - \chi'_{\mathrm{GT}}$ and $\tilde{\chi}_F = 2\chi'_F - \chi_F$. Also here, as in Table I, all calculations are in good (Ge-Se-Te-Xe) or fair (Mo-Nd-Sm) agreement. NLO corrections, not shown in Table II, also appear to be small. The main result of this subsection is therefore that NLO corrections appear to be small for all matrix elements and they will be henceforth neglected.

B. Neutrinoless double-β decay matrix elements in IBM-2

Very recently, another formulation of nuclear matrix elements in neutrinoless double-β decay has been put forward recently by Šimkovic *et al.* [10]. We use this formulation from here onward to compare IBM-2 results with recent results from the SM and QRPA. This formulation agrees with that of Tomoda for F and GT matrix elements, but it adds other contributions, denoted by HOC. The transition operator is now

TABLE I. Dependence of neutrinoless double-β decay nuclear matrix elements on approximations GS, IBM-2, IBM-2 NLO in the formulation of Ref. [9]. The calculations of SM [7] and QRPA [9] are shown for comparison. All matrix elements in fm^{-1}.

		SM	QRPA	GS	IBM-2	IBM-2 NLO
$M_{\rm GT}^{(0\nu)}$ (fm^{-1})	^{76}Ge $\rightarrow$ ^{76}Se	0.411	0.330	0.553	0.446	0.450
	^{82}Se $\rightarrow$ ^{82}Kr	0.331	0.293	0.416	0.346	0.348
	^{100}Mo $\rightarrow$ ^{100}Ru		0.316	0.392	0.338	0.336
	^{128}Te $\rightarrow$ ^{128}Xe	0.412	0.246	0.435	0.318	0.319
	^{130}Te $\rightarrow$ ^{130}Xe	0.413	0.212	0.382	0.285	0.286
	^{136}Xe $\rightarrow$ ^{136}Ba		0.117	0.293		
	^{150}Nd $\rightarrow$ ^{150}Sm		0.312	0.220	0.183	0.173
	^{154}Sm $\rightarrow$ ^{154}Gd			0.291	0.197	0.176
$M_{F}^{(0\nu)}$ (fm^{-1})	^{76}Ge $\rightarrow$ ^{76}Se	-0.129	-0.150	-0.318	-0.249	-0.251
	^{82}Se $\rightarrow$ ^{82}Kr	-0.092	-0.131	-0.264	-0.211	-0.212
	^{100}Mo $\rightarrow$ ^{100}Ru		-0.165	-0.034	-0.029	-0.026
	^{128}Te $\rightarrow$ ^{128}Xe	-0.145	-0.114	-0.219	-0.157	-0.158
	^{130}Te $\rightarrow$ ^{130}Xe	-0.145	-0.099	-0.191	-0.139	-0.140
	^{136}Xe $\rightarrow$ ^{136}Ba		-0.058	-0.140		
	^{150}Nd $\rightarrow$ ^{150}Sm		-0.154	-0.026	-0.022	-0.020
	^{154}Sm $\rightarrow$ ^{154}Gd			-0.031	-0.020	-0.017
$M^{(0\nu)}$ (fm^{-1})	^{76}Ge $\rightarrow$ ^{76}Se	0.494	0.426	0.756	0.606	0.610
	^{82}Se $\rightarrow$ ^{82}Kr	0.390	0.377	0.585	0.481	0.484
	^{100}Mo $\rightarrow$ ^{100}Ru		0.422	0.414	0.357	0.353
	^{128}Te $\rightarrow$ ^{128}Xe	0.505	0.319	0.575	0.418	0.420
	^{130}Te $\rightarrow$ ^{130}Xe	0.506	0.275	0.504	0.374	0.375
	^{136}Xe $\rightarrow$ ^{136}Ba		0.154	0.383		
	^{150}Nd $\rightarrow$ ^{150}Sm		0.411	0.237	0.197	0.186
	^{154}Sm $\rightarrow$ ^{154}Gd			0.311	0.210	0.187

TABLE II. IBM-2 matrix elements of terms nonproportional to the neutrino mass-squared operator in the formulation of Ref. [9]. The calculations of SM [7] and QRPA [9] are also shown. All matrix elements in fm^{-1}.

		SM	QRPA	IBM-2		SM	QRPA	IBM-2
$M_{\rm GT}^{(0\nu)}$ (fm^{-1})	^{76}Ge $\rightarrow$ ^{76}Se	0.411	0.330	0.446	^{130}Te $\rightarrow$ ^{130}Xe	0.413	0.212	0.285
	^{82}Se $\rightarrow$ ^{82}Kr	0.331	0.293	0.346	^{136}Xe $\rightarrow$ ^{136}Ba		0.117	
	^{100}Mo $\rightarrow$ ^{100}Ru		0.316	0.338	^{150}Nd $\rightarrow$ ^{150}Sm		0.312	0.183
	^{128}Te $\rightarrow$ ^{128}Xe	0.412	0.246	0.318	^{154}Sm $\rightarrow$ ^{154}Gd			0.197
χ_F	^{76}Ge $\rightarrow$ ^{76}Se	-0.200	-0.290	-0.357	^{130}Te $\rightarrow$ ^{130}Xe	-0.225	-0.299	-0.313
	^{82}Se $\rightarrow$ ^{82}Kr	-0.177	-0.286	-0.389	^{136}Xe $\rightarrow$ ^{136}Ba		-0.317	
	^{100}Mo $\rightarrow$ ^{100}Ru		-0.334	-0.056	^{150}Nd $\rightarrow$ ^{150}Sm		-0.316	-0.076
	^{128}Te $\rightarrow$ ^{128}Xe	-0.225	-0.296	-0.316	^{154}Sm $\rightarrow$ ^{154}Gd			-0.064
$\chi'_{\rm GT}$	^{76}Ge $\rightarrow$ ^{76}Se	1.141	1.049	1.180	^{130}Te $\rightarrow$ ^{130}Xe	1.179	1.052	1.226
	^{82}Se $\rightarrow$ ^{82}Kr	1.142	1.048	1.189	^{136}Xe $\rightarrow$ ^{136}Ba		1.026	
	^{100}Mo $\rightarrow$ ^{100}Ru		1.032	1.177	^{150}Nd $\rightarrow$ ^{150}Sm		1.057	1.184
	^{128}Te $\rightarrow$ ^{128}Xe	1.175	1.049	1.218	^{154}Sm $\rightarrow$ ^{154}Gd			1.200
χ'_F	^{76}Ge $\rightarrow$ ^{76}Se	-0.231	-0.318	-0.426	^{130}Te $\rightarrow$ ^{130}Xe	-0.271	-0.331	-0.388
	^{82}Se $\rightarrow$ ^{82}Kr	-0.204	-0.314	-0.469	^{136}Xe $\rightarrow$ ^{136}Ba		-0.349	
	^{100}Mo $\rightarrow$ ^{100}Ru		-0.363	-0.058	^{150}Nd $\rightarrow$ ^{150}Sm		-0.352	-0.082
	^{128}Te $\rightarrow$ ^{128}Xe	-0.272	-0.326	-0.389	^{154}Sm $\rightarrow$ ^{154}Gd			-0.069
χ'_T	^{76}Ge $\rightarrow$ ^{76}Se	-0.013	-0.230	-0.134	^{130}Te $\rightarrow$ ^{130}Xe	-0.025	-0.231	-0.101
	^{82}Se $\rightarrow$ ^{82}Kr	-0.021	-0.248	-0.172	^{136}Xe $\rightarrow$ ^{136}Ba		-0.221	
	^{100}Mo $\rightarrow$ ^{100}Ru		-0.470	0.130	^{150}Nd $\rightarrow$ ^{150}Sm		-0.333	0.110
	^{128}Te $\rightarrow$ ^{128}Xe	-0.030	-0.226	-0.103	^{154}Sm $\rightarrow$ ^{154}Gd			0.116

TABLE III. Evolution of the different HOC in the ^{76}Ge $\rightarrow$ ^{76}Se neutrinoless matrix elements (in fm^{-1}) calculated in IBM-2 as we add the FNS and the SRC corrections.

Fermi matrix elements $[M_F^{(0\nu)}]$					
	$AA+VV$	AP	PP	MM	Sum
Bare	−0.2845	0.0000	0.0000	0.0000	−0.2845
+FNS	−0.2640	0.0000	0.0000	0.0000	−0.2640
+SRC	−0.2557	0.0000	0.0000	0.0000	−0.2557
+FNS+SRC	−0.2487	0.0000	0.0000	0.0000	−0.2487
Gamow-Teller matrix elements $[M_{\rm GT}^{(0\nu)}]$					
	$AA+VV$	AP	PP	MM	Sum
Bare	0.5418	−0.1164	0.0346	0.0362	0.4962
+FNS	0.5032	−0.0959	0.0262	0.0221	0.4557
+SRC	0.4548	−0.0734	0.0166	−0.0008	0.3973
+FNS+SRC	0.4464	−0.0714	0.0168	0.0111	0.4029
Tensor matrix elements $[M_T^{(0\nu)}]$					
	$AA+VV$	AP	PP	MM	Sum
Bare	0.0000	−0.0367	0.0120	−0.0061	−0.0308
+FNS	0.0000	−0.0296	0.0090	−0.0038	−0.0243
+SRC	0.0000	−0.0367	0.0119	−0.0053	−0.0300
+FNS+SRC	0.0000	−0.0299	0.0092	−0.0038	−0.0246
$M^{(0\nu)} = -(\frac{g_V}{g_A})^2 M_F^{(0\nu)} + M_{\rm GT}^{(0\nu)} + M_T^{(0\nu)}$					
	$AA+VV$	AP	PP	MM	Sum
Bare	0.7239	−0.1531	0.0466	0.0301	0.6475
+FNS	0.6722	−0.1255	0.0353	0.0184	0.6004
+SRC	0.6185	−0.1101	0.0286	−0.0061	0.5309
+FNS+SRC	0.6056	−0.1014	0.0260	0.0073	0.5376

written in momentum space as

$$H(p) = -h^F(p) + h^{\rm GT}(p)\vec{\sigma}_n \cdot \vec{\sigma}_{n'} + h^T(p)S^p_{nn'} \quad (35)$$

with

$$h^F(p) = h^F_{VV}(p), \quad (36)$$

$$h^{\rm GT}(p) = h^{\rm GT}_{AA}(p) + h^{\rm GT}_{AP}(p) + h^{\rm GT}_{PP}(p) + h^{\rm GT}_{MM}(p), \quad (37)$$

$$h^T(p) = h^T_{AP}(p) + h^T_{PP}(p) + h^T_{MM}(p). \quad (38)$$

Compared with Tomoda's formulation, the tensor operator is defined with an extra factor of 3

$$S^p_{nn'} = 3[(\vec{\sigma}_n \cdot \hat{p})(\vec{\sigma}_{n'} \cdot \hat{p})] - \vec{\sigma}_n \cdot \vec{\sigma}_{n'} \quad (39)$$

and the matrix elements are defined without the factor $\frac{1}{2}$ in front. The form of the different terms in the potentials are given explicitly in Appendix A. Because our formalism is general enough, we can evaluate the matrix elements also in this formulation and study the effects of the new contributions h_{AP}, h_{PP}, h_{MM}, as done recently by Menéndez *et al.* [19] and by Šimkovic *et al.* [20]. This study is shown in Table III for the decay ^{76}Ge $\rightarrow$ ^{76}Se. The overall calculations are shown in Table IV.

Our results, expressed in units of fm^{-1} in the previous tables, are multiplied in Table IV by $2R$, where $R = 1.2A^{1/3}$ is the nuclear radius in fm, to compare them with the calculations of Refs. [19,20]. Our results are in agreement with the QRPA results but disagree with the SM results by a factor of 2. This is shown in Fig. 2. The agreement with QRPA, especially in the behavior of the matrix elements with mass number A, is somewhat surprising because the two methods (QRPA and IBM-2) are very different. One of the major sources of

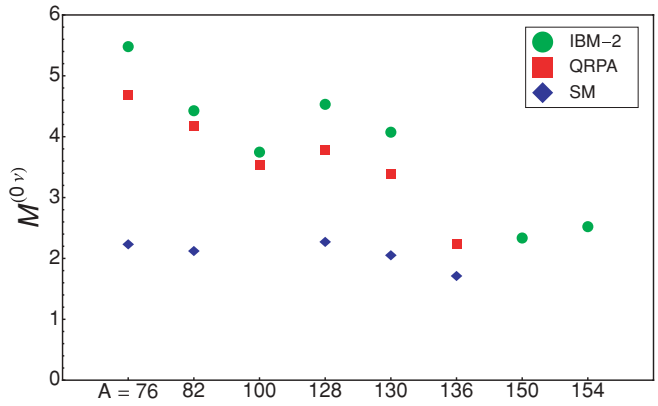

FIG. 2. (Color online) Neutrinoless double-β decay matrix elements in the formulation of Šimkovic *et al.* [10] for IBM-2, Set I (this work), QRPA with $g_A = 1.25$ and Jastrow SRC [20], and SM [8].

TABLE IV. Neutrinoless nuclear matrix elements to ground state including HOC calculated in IBM-2, SM [8], and QRPA [20] (last three columns). Previous three columns show the break down in F, GT and T contribution to IBM 2. All matrix elements in dimensionless units.

	IBM-2			IBM-2	QRPA	SM
	$M_F^{(0\nu)}$	$M_{\rm GT}^{(0\nu)}$	$M_T^{(0\nu)}$		$M^{(0\nu)}$	
^{76}Ge $\rightarrow$ ^{76}Se	−2.529	4.096	−0.250	5.465	4.680	2.220
^{82}Se $\rightarrow$ ^{82}Kr	−2.197	3.260	−0.254	4.412	4.170	2.110
^{100}Mo $\rightarrow$ ^{100}Ru	−0.327	3.318	0.204	3.732	3.530	
^{128}Te $\rightarrow$ ^{128}Xe	−1.897	3.463	−0.161	4.517	3.770	2.260
^{130}Te $\rightarrow$ ^{130}Xe	−1.693	3.119	−0.144	4.059	3.380	2.040
^{136}Xe $\rightarrow$ ^{136}Ba					2.220	1.700
^{150}Nd $\rightarrow$ ^{150}Sm	−0.279	2.034	0.108	2.321		
^{154}Sm $\rightarrow$ ^{154}Gd	−0.255	2.226	0.118	2.507		

disagreement with the SM is the magnitude of the Fermi matrix elements, which is much smaller in the SM than in our calculation.

We can, of course, also calculate matrix elements to any excited 0^+ state and we give for completeness in Table V the matrix elements to the first excited 0^+ states in the daughter nuclei. Although these matrix elements in many cases are comparable to those to the ground state, in practice decay to the excited states is reduced by the phase-space factor $G_{0\nu}$ of Eq. (1).

C. Sensitivity of IBM-2 results to parameter changes

We have investigated the sensitivity of our results to parameter changes. We begin with the study of the sensivity to the single-particle energies. We show in Table VI a comparison between the results using Set I, with energies extracted from experiment and thus called *experimental*, and Set II obtained from a calculation in a Woods-Saxon well and thus called *theoretical*. Both sets of single-particle energies are given in Appendix B. We observe a 15% decrease of the matrix elements in Ge-Se-Te and a 15% increase in Mo-Nd-Sm when going from Set I to Set II. This is due to the interplay of two effects: (i) in Set II the high-j orbitals are at an higher excitation energy than in Set I and (ii) while in Ge-Se-Te protons and neutrons are in the same major shell, in Mo-Nd-Sm they are in different shells. The decrease-increase is due to the magnitude and phase of the contribution of high-j "intruder" orbitals relative to "normal" orbitals. We note that the results with Set II are in perfect agreement with QRPA results, $g_A = 1.25$, Jastrow correlations, for Ge-Se-Te, whereas for Mo the QRPA result is more in agreement with our Set I. The importance of energies and occupancies of single-particle states in double-β decay has been stressed recently by Schiffer *et al.* [21].

Also, in a recent article [22], it has been shown that in the QRPA calculation of ^{76}Ge decay, the use of single-particle energies that reproduce measured occupation probabilities reduce the double-β decay matrix element from its value with "theoretical" single-particle energies, in contrast with our result. The "theoretical" single-particle energies used in Ref. [22], called WS, are identical to our Set II. The calculated values from Table VI are IBM-2 (II), 4.636, and QRPA, 4.680, in surprising agreement. Our "experimental" Set I differs from the "theoretical" Set II by a lowering of the high-spin orbital $1g_{9/2}$ (see Table XI) in agreement with the observed occupation probabilities quoted in Ref. [22]. The different behavior between IBM-2 and QRPA in ^{76}Ge, when going from "theoretical" to "experimental," is probably due to a change in parameters other than single-particle energies in QRPA.

We have also investigated the sensitivity to other parameters in the calculation of ^{76}Ge decay. The sensitivity of individual matrix elements M_F, $M_{\rm GT}$, and M_T to changes in the strength A_1 of the SDI that generates the correlated pairs is shown in the top part of Table VII. The "standard" value of A_1 is $25/A$ with a reasonable range of variation of $\pm 10\%$ (for ^{76}Ge,

TABLE V. Neutrinoless matrix elements to first excited 0^+ state including HOC calculated in IBM-2. All matrix elements in dimensionless units.

	$M_F^{(0\nu)}$	$M_{\rm GT}^{(0\nu)}$	$M_T^{(0\nu)}$	$M^{(0\nu)}$
^{76}Ge $\rightarrow$ ^{76}Se	−1.212	1.805	−0.102	2.479
^{82}Se $\rightarrow$ ^{82}Kr	−0.688	0.860	−0.053	1.247
^{100}Mo $\rightarrow$ ^{100}Ru	−0.034	0.380	0.017	0.419
^{128}Te $\rightarrow$ ^{128}Xe	−1.402	2.444	−0.099	3.243
^{130}Te $\rightarrow$ ^{130}Xe	−1.321	2.332	−0.088	3.090
^{150}Nd $\rightarrow$ ^{150}Sm	−0.046	0.349	0.016	0.395
^{154}Sm $\rightarrow$ ^{154}Gd	−0.009	0.010	0.006	0.021

TABLE VI. Comparison between matrix elements $M^{(0\nu)}$ calculated with Set I and Set II of single-particle energies in IBM-2. QRPA [20] and SM [8] are also shown. All matrix elements in dimensionless units.

	IBM-2 (I)	IBM-2 (II)	QRPA	SM
^{76}Ge $\rightarrow$ ^{76}Se	5.465	4.636	4.680	2.220
^{82}Se $\rightarrow$ ^{82}Kr	4.412	3.805	4.170	2.110
^{100}Mo $\rightarrow$ ^{100}Ru	3.732	4.217	3.530	
^{128}Te $\rightarrow$ ^{128}Xe	4.517	3.845	3.770	2.260
^{130}Te $\rightarrow$ ^{130}Xe	4.059	3.372	3.380	2.040
^{150}Nd $\rightarrow$ ^{150}Sm	2.321	2.888		
^{154}Sm $\rightarrow$ ^{154}Gd	2.507	3.094		

TABLE VII. a. Sensitivity of the matrix elements (in fm^{-1}) of the ^{76}Ge decay to changes in the surface delta interaction strength A_1 (in MeV).

A_1	$M_F^{(0\nu)}$	$M_{\mathrm{GT}}^{(0\nu)}$	$M_T^{(0\nu)}$	$M^{(0\nu)}$
0.30	−0.241	0.394	−0.024	0.524
0.35	−0.262	0.431	−0.025	0.574
0.40	−0.279	0.460	−0.027	0.612

b. Sensitivity of the matrix elements (in fm^{-1}) of the ^{76}Ge decay to changes in the oscillator parameter ν_0 (in fm^{-2}).

ν_0	$M_F^{(0\nu)}$	$M_{\mathrm{GT}}^{(0\nu)}$	$M_T^{(0\nu)}$	$M^{(0\nu)}$
0.8	−0.224	0.369	−0.021	0.491
1.0	−0.249	0.404	−0.025	0.538
1.2	−0.271	0.432	−0.028	0.577

c. Sensitivity of the matrix elements (in fm^{-1}) of the ^{76}Ge decay to changes in the closure energy $\tilde{A}$ (in MeV).

	$M_F^{(0\nu)}$	$M_{\mathrm{GT}}^{(0\nu)}$	$M_T^{(0\nu)}$	$M^{(0\nu)}$
5	−0.275	0.445	−0.025	0.596
10	−0.246	0.398	−0.024	0.531
15	−0.224	0.364	−0.024	0.483

$25/A = 0.33$). The sensitivity within this range appears to be small. We expect to have the same minor sensitivity also to changes in the interaction. In fact, if the interaction is chosen in such a way as to reproduce the $0^+ - 2^+$ energy difference, as it should in any realistic calculation, we expect very small differences, if any at all.

The sensitivity to the parameter ν_0 that appears in the oscillator size as $\nu = \nu_0 A^{-1/3}$ is shown in the central part of Table VII. The value we have used is $\nu_0 = 0.994\ \mathrm{fm}^{-2}$. A reasonable range of variation is ±5%. Within this range the sensitivity is small [larger ν, larger $M^{(0\nu)}$].

Finally, in the bottom part of Table VII, we show the sensitivity to the closure energy, $\tilde{A}$. We find, in accordance with other calculations, that this sensitivity is small and thus the closure approximation is good.

The main source of uncertainty in the calculation is the Gamow-Teller strength g_A. It is very well known that, in single-β decay, this strength is quenched to 70% of its free value $g_A = 1.25$. Studies of double-β decay with the emission of two neutrinos also indicate a quenching of similar amount. (We have done similar studies and we will report them in a subsequent article). Quenching is extremely important for double-β decay because g_A appears to the fourth power, g_A^4, in the decay rate. The origin of the quenching is not completely known. If it occurs also for neutrinoless double-β decay, it would considerably reduce the values given above by as much as a factor of 4.

VI. SIMPLE FEATURES OF THE CALCULATION

A. Mass dependence

To study the mass dependence of $M^{(0\nu)}$ we plot our results in Fig. 3 as a function of mass number A. By fitting these

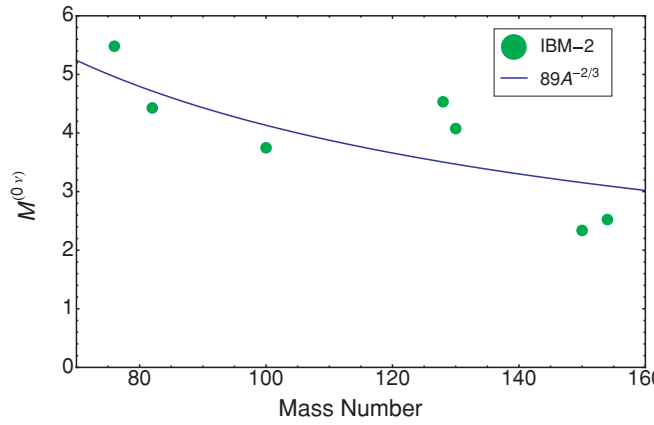

FIG. 3. (Color online) Overall A dependence of the matrix elements $M^{(0\nu)}$ in IBM-2, Set I, fitted with the empirical formula of Eq. (40).

results with a dependence $M^{(0\nu)} = M_0 A^{-2/3}$ we find

$$M^{(0\nu)} \simeq 89 A^{-2/3}. \tag{40}$$

Converting to fm^{-1} by dividing by $2R$, we find

$$M^{(0\nu)}(\mathrm{fm}^{-1}) \simeq 37/A. \tag{41}$$

The same dependence appears in the QRPA results but not in the SM results. The dimensionless matrix elements in the SM appear to be independent of A and always ∼2, a surprising result.

B. Shell effects

To study shell effects, we plot in Fig. 4 our results as a function of neutron number. Shell effects can be simply studied within the framework of the generalized seniority scheme. In Fig. 5 we plot a calculation of neutrinoless double-β decay matrix elements for all Te isotopes. (Of course, the $Q_{\beta\beta}$ value is positive only for ^{128}Te and ^{130}Te.) The behavior of Fig. 5 can be simply understood by considering the first term in the boson mapping $A_\pi A_\nu s_\pi^\dagger \tilde{s}_\nu$. This is simply the operator

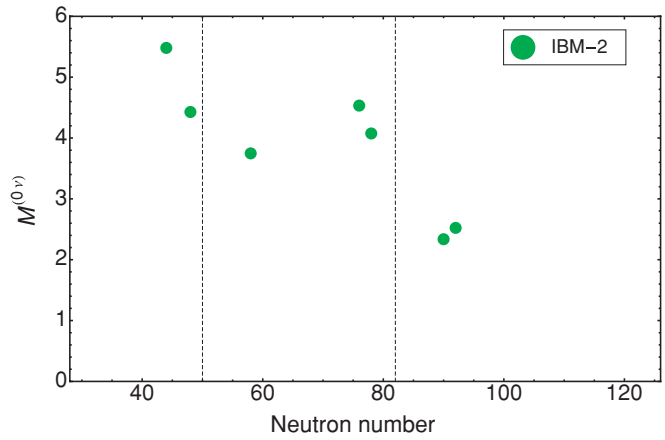

FIG. 4. (Color online) Dependence of the matrix elements in IBM-2, Set I, on neutron number in the shells 28–50, 50–82 and 82–126.

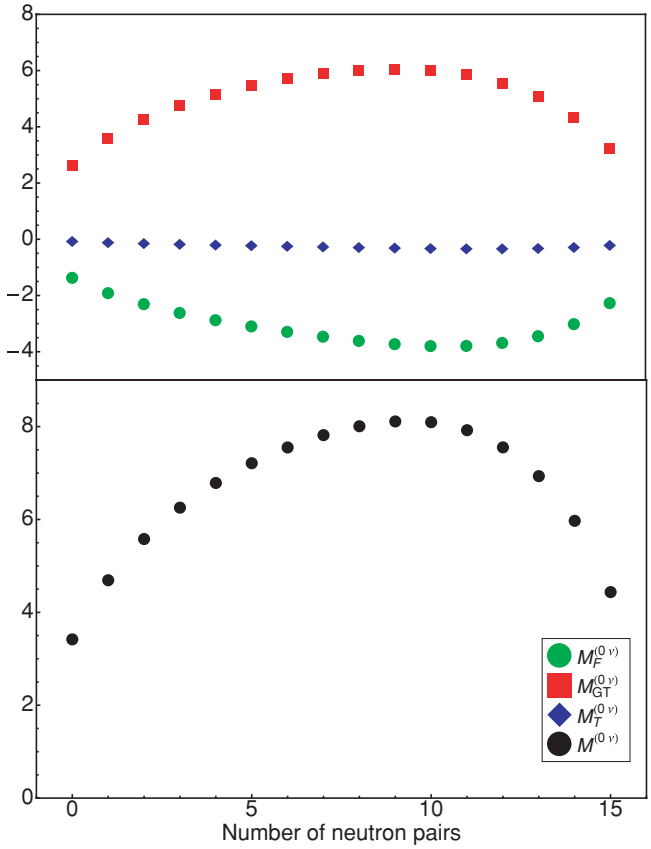

FIG. 5. (Color online) Dependence of the calculated matrix elements on the number of valence neutron pairs in the GS scheme. (Top panel) $M_F^{(0\nu)}$, $M_{\rm GT}^{(0\nu)}$, and $M_T^{(0\nu)}$. (Bottom panel) The total matrix element $M^{(0\nu)}$.

that annihilates a correlated pair of neutrons and creates a correlated pair of protons. This operator can be written, to a good approximation, as [23]

$$P^{(0)}_{+\pi} P^{(0)}_{-\nu} = \alpha_\pi \alpha_\nu s^\dagger_\pi \left(\Omega_\pi - N_\pi\right)^{1/2} \left(\Omega_\nu - N_\nu\right)^{1/2} \tilde{s}_\nu, \quad (42)$$

where Ω_π and Ω_ν are the pair degeneracies of the major shells and N_π and N_ν are the boson numbers (numbers of pairs). The matrix elements of the operator in Eq. (42) are

$$\langle N_\pi + 1, N_\nu - 1 \left| P^{(0)}_{+\pi} P^{(0)}_{-\nu} \right| N_\pi, N_\nu \rangle = \alpha_\pi \alpha_\nu \sqrt{(N_\pi + 1)(\Omega_\pi - N_\pi)(\Omega_\nu - N_\nu + 1) N_\nu}. \quad (43)$$

The coefficients α_π, α_ν are characteristic quantities of each major shell. The behavior (43) is shown in Fig. 6. (This is slightly different from the realistic calculation of Fig. 5 obtained with single-particle levels for protons slightly different than for neutron.) Equation (43) provides a simple estimate of $M^{(0\nu)}$. As an example of application of Eq. (43), consider the ratio $^{128}_{52}\mathrm{Te}_{76}/^{130}_{52}\mathrm{Te}_{78}$. For Te, protons and neutrons are in the 50–82 shell, $\Omega_\pi = \Omega_\nu = 16$ and $N_\pi = 1$ and $N_\nu = 13(^{128}\mathrm{Te})$, $N_\nu = 14$ (^{130}Te). From (43) one obtains

$$\frac{M^{(0\nu)}(^{128}\mathrm{Te})}{M^{(0\nu)}(^{130}\mathrm{Te})} = 1.11. \quad (44)$$

The result of our calculation (IBM-2 in Table IV) gives $M^{(0\nu)}(^{128}\mathrm{Te})/M^{(0\nu)}(^{130}\mathrm{Te}) = \frac{4.517}{4.059} = 1.11$. This calculation includes FSC and SRC effects. Formula (43), derived in GS and spherical nuclei, appears also to be valid for the full calculation (IBM-2) and weakly deformed nuclei. The analogy between neutrinoless double-β decay and $2n$ and $2p$ transfer suggests that the physical decay occurs in a correlated pair and is thus enhanced by pairing correlations. It also allows a *model-independent* prediction for ratios of matrix elements, by resorting to experimental data for $2n$ (and $2p$) transfer reactions

$$^A_Z X_N(p,t)\, ^A_Z X_{N-2}. \quad (45)$$

The intensities of these reactions are proportional to the square of the matrix elements of the operator $P^{(0)}_{-\nu}$ and thus, for fixed proton number, to the square of the matrix elements $M^{(0\nu)}$. As reported in Ref. [23], the experimental two-neutron transfer reactions in Te appear to be well described by Eq. (43).

The relation described above is also well satisfied by QRPA. For example, from Table IV, row QRPA, we have $M^{(0\nu)}(^{128}\mathrm{Te})/M^{(0\nu)}(^{130}\mathrm{Te}) = \frac{3.770}{3.338} = 1.13$.

We suggest that the relation

$$M^{(0\nu)} \simeq \alpha_\pi \alpha_\nu \sqrt{N_\pi + 1}\sqrt{N_\nu}\sqrt{\Omega_\pi - N_\pi}\sqrt{\Omega_\nu - N_\nu + 1} \quad (46)$$

be used to estimate $M^{(0\nu)}$ for spherical and weakly deformed nuclei with $A \gtrsim 60$. By fitting our calculation in ^{76}Ge with (43) we find $\alpha_\pi \alpha_\nu = 0.186$ for protons and neutrons in the 28–50 shell and by fitting in ^{128}Te we find $\alpha_\pi \alpha_\nu = 0.114$ for protons and neutrons in the 50–82 shell. These values are used in Fig. 6, where also the two points ^{128}Te and ^{130}Te are shown.

As mentioned above, this estimate applies to spherical and weakly deformed nuclei. For strongly deformed nuclei, it should be modified as discussed in Ref. [23].

C. Effects of deformation

The effects of deformation can be easily seen within the microscopic IBM framework. In spherical nuclei, the ground state is composed of S pairs (s bosons) and is well described by generalized seniority. As the deformation increases, the number of d-bosons in the ground state increases, reaching a maximum of $(2/3)(N_\pi + N_\nu)$ in SU(3) nuclei. The effects of the deformation are the differences between the rows GS and IBM-2 in Table I. For the nuclei described in this article, the effect is a reduction by about 20%. The advantage of the method discussed in this article is that one can do calculations in any nucleus with $A \gtrsim 70$. For semimagic nuclei, one can use GS, whereas for all others one can use IBM-2. To study further the effects of strong defomation, we are planning to calculate the matrix elements in the decay of ^{160}Gd, ^{232}Th, and ^{238}U, for which we need first to obtain realistic wave functions that describe accurately all observed properties. The results of the calculation will be presented in a forthcoming publication.

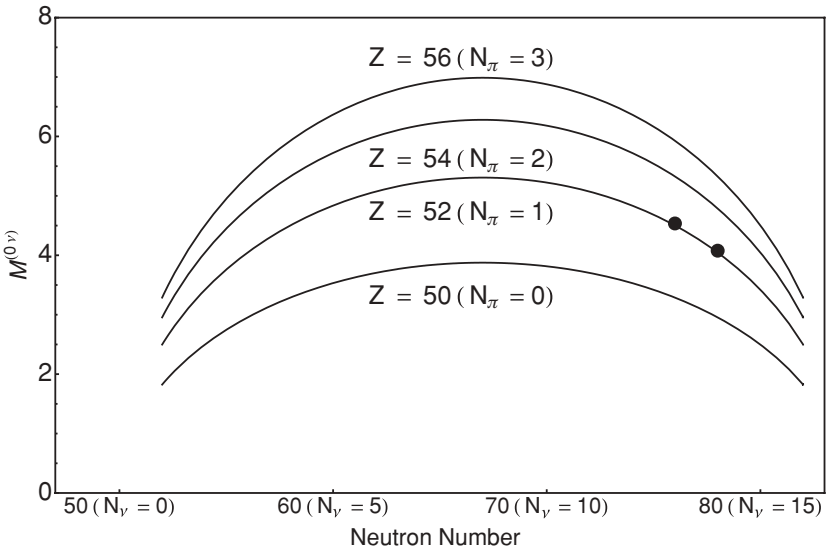

FIG. 6. Behavior of the matrix elements $M^{(0\nu)}$ for protons and neutrons in the shell 50–82 using Eq. (46) with $\alpha_\pi \alpha_\nu = 0.114$. The points correspond to the IBM-2 results of the ^{128,130}Te decays.

VII. CONCLUSIONS

In this article we have presented a formalism for calculating matrix elements of double-β decay within the framework of the microscopic interacting boson model and applied it to the decays of ^{76}Ge, ^{82}Se, ^{100}Mo, ^{128}Te, ^{130}Te, ^{136}Xe, ^{150}Nd, and ^{154}Sm. This calculation provides an alternative to the SM and the QRPA. The results of our calculations are in agreement with QRPA both for the Tomoda formulation and for the Šimkovic formulation ($g_A = 1.25$, Jastrow SRC). They are in disagreement with recent large scale shell-model calculations that are a factor of two smaller and show no A dependence. The origin of this disagreement is not clear. In IBM-2, we include both the effects of high seniority states up to a maximum of $2(N_\pi + N_\nu)$, in ^{128}Te, for example, up to $v = 8$, and the effects of deformation up to quadrupole deformation (d bosons). The only missing part is the effect of high-J (hexadecapole, etc.) pairs. However, in the 1980s these were estimated to be small in weakly deformed nuclei, reaching a maximum of about 10% in strongly deformed nuclei. Because the calculations are very complex and each introduces approximations, we cannot exclude that there are errors both in the formulation and in the calculation, especially because there are several formulations and several calculations with different parameter assumptions. It would be of great importance, as emphasized by the late John Bahcall [24], to bring all methods SM, QRPA (and now IBM-2) to results that differ only by the sensitivity to parameters, i.e., of the order of 20%. The agreement between IBM-2 and QRPA, both in absolute value and in their A dependence, is somewhat surprising because these two methods start from rather different assumptions. In IBM-2, one starts from correlated S and D pairs of identical nucleons and includes the effects of the deformation through the bosonic neutron-proton quadrupole interaction. In QRPA, one starts from S pairs in the BCS approximation and includes other effects through quasiparticle interactions. It appears that for spherical and weakly deformed nuclei both methods produce the same result. To understand further how far the agreement extends, it would be interesting to compare QRPA with our results in ^{150}Nd (a weakly deformed nucleus) and ^{154}Sm. Although IBM-2 calculations can easily proceed beyond the spherical-deformed transition region into the strongly deformed region [17], QRPA must address the problem of its instabilities.

In addition to its ability to attack strongly deformed nuclei, another important point of the IBM-2 calculation is that it makes use of *realistic* wave functions, that is, wave functions that describe well the experimental data on spectra, electromagnetic transition, and two-nucleon transfer reaction rates. Perhaps to further understand the differences between various calculations, it would be useful to see how well the SM and QRPA wave functions describe available data. The disagreement between IBM-2 and SM is particularly troublesome, because IBM-2 is a truncation of the shell-model space to the S and D pair space and, in the limit of spherical nuclei, IBM-2 and SM should produce the same results.

From the IBM-2 point of view we are planning to extend our calculation to more nuclei, in particular to nuclei in the strongly deformed region, ^{160}Gd, ^{232}Th, and ^{238}U. The extension to other isotopes of Sm, Nd, Xe, Mo, Se as well as to Ru and Cd is straightforward because realistic wave function were obtained in the 1980s [17] and are readable available.

ACKNOWLEDGMENTS

This work was performed in part under DOE Grant No. DE-FG-02-91ER40608 and supported in part by Ministerio de Ciencia y Innovación (Spain) under contract No. FIS2008-04189.

APPENDIX A: EVALUATION OF THE RADIAL INTEGRALS

The two-body matrix elements of $V^{(\lambda)}_{s_1 s_2}$ between two-fermion states contain the radial integrals $R^{(k_1,k_2,\lambda)}(n_1, l_1, n_2, l_2; n'_1, l'_1, n'_2, l'_2)$. Since the potentials for neutrinoless double-β decay are best given in momentum space, we compute the

TABLE VIII. Neutrino potentials $V(r)$ in configuration and momentum space for the different types of $\beta\beta$ transitions. $\tilde{A} = \langle E_N \rangle - (E_I + E_F)/2$ is the closure energy.

Transition	V	Quantum no.		$V(r)$	$v_\lambda(p)$
		λ	$s_1 = s_2$		
$2\nu\beta\beta$ Fermi	$V_F^{(2\nu)}$	0	0	1	$\frac{\delta(p)}{p^2}$
$2\nu\beta\beta$ Gamow-Teller	$V_{\rm GT}^{(2\nu)}$	0	1		
$0\nu\beta\beta$ Fermi	$V_F^{(0\nu)}$	0	0	$H(r)$	$\frac{2}{\pi}\frac{1}{p(p+\tilde{A})}$
$0\nu\beta\beta$ Gamow-Teller	$V_{\rm GT}^{(0\nu)}$	0	1		
$0\nu\beta\beta$ Fermi	$V_F^{\prime(0\nu)}$	0	0	$-rH'(r)$	$\frac{2}{\pi}\frac{p+2\tilde{A}}{p(p+\tilde{A})^2}$
$0\nu\beta\beta$ Gamow-Teller	$V_{\rm GT}^{\prime(0\nu)}$	0	1		
$0\nu\beta\beta$ Fermi	$\tilde{V}_F^{(0\nu)}$	0	0	$\tilde{H}(r) = 2H(r) + rH'(r)$	$\frac{2}{\pi}\frac{1}{(p+\tilde{A})^2}$
$0\nu\beta\beta$ Gamow-Teller	$\tilde{V}_{\rm GT}^{(0\nu)}$	0	1		
$0\nu\beta\beta$ Tensor	$V_T^{(0\nu)}$	2	1	$-rH'(r)$	$\frac{2}{\pi}\frac{2p+\tilde{A}}{p(p+\tilde{A})^2}$

radial integrals in this space

$$R^{(k_1,k_2,\lambda)}(n_1,l_1,n_2,l_2,n_1',l_1',n_2',l_2') = \int_0^\infty v_\lambda(p)p^2dp \int_0^\infty R_{n_1l_1}(r_1)R_{n_1'l_1'}(r_1)j_{k_1}(pr_1)r_1^2dr_1 \times \int_0^\infty R_{n_2l_2}(r_2)R_{n_2'l_2'}(r_2)j_{k_2}(pr_2)r_2^2dr_2, \quad \text{(A1)}$$

where $R_{nl}(r)$ is the radial part of the wave function associated with a single-particle state nl and $v_\lambda(p)$ is the Fourier-Bessel transform of the potential

$$v_\lambda(p) = \frac{2}{\pi}\int_0^\infty V(r)j_\lambda(pr)r^2dr. \quad \text{(A2)}$$

The radial matrix elements can then be evaluated in closed form with harmonic oscillator single particle wave functions by using the Horie method [25] and are given by

$$R^{(k_1,k_2,\lambda)}(n_1,l_1,n_2,l_2,n_1',l_1',n_2',l_2') = \left[M_{n_1l_1}M_{n_1'l_1'}M_{n_2l_2}M_{n_2'l_2'}\right]^{-\frac{1}{2}} \times \sum_{s_1=0}^{n_1+n_1'}\sum_{s_2=0}^{n_2+n_2'} f^{(k_1k_2\lambda)}(l_1+l_1'+2s_1, l_2+l_2'+2s_2) \times a_{l_1+l_1'+2s_1}(n_1l_1;n_1'l_1')a_{l_2+l_2'+2s_2}(n_2l_2;n_2'l_2'), \quad \text{(A3)}$$

where $M_{nl} = 2^n n!(2n+2l+1)!!$ and

$$a_{l+l'+2s}(nl;n'l') = (-1)^s\sum_{\mu=0}^{n}\binom{n}{\mu}\binom{n'}{s-\mu} \times \frac{(2n+2l+1)!!}{(2\mu+2l+1)!!}\frac{(2n'+2l'+1)!!}{(2(s-\mu)+2l'+1)!!}, \quad \text{(A4)}$$

$$f^{(k_1k_2\lambda)}(m_1,m_2) = \sum_{m=\frac{k_1+k_2}{2}}^{\frac{m_1+m_2}{2}} a_{2m}\left(\frac{m_1-k_1}{2}k_1;\frac{m_2-k_2}{2}k_2\right) \times J_m^{(\lambda)}(\nu), \quad \text{(A5)}$$

with

$$J_m^{(\lambda)}(\nu) = (2\nu)^{-m}\int_0^\infty v_\lambda(p)e^{-\frac{p^2}{2\nu}}p^{2m+2}dp. \quad \text{(A6)}$$

Here $\nu = M\omega/\hbar$ is the harmonic oscillator parameter with M the nucleon mass. The integrals $J_m^{(\lambda)}(\nu)$ are the Horie intergrals related to the Talmi integrals. In those cases in which the potential is given in configuration space, they can be expressed as

$$J_m^{(\lambda)}(\nu) = \sum_{\mu=0}^{\frac{2m-\lambda}{2}}(-1)^\mu\binom{\frac{2m-\lambda}{2}}{\mu}\frac{(2m+\lambda+1)!!}{2^m(2\lambda+2\mu+1)!!} \times \sqrt{\frac{2}{\pi}}\nu^{\frac{\lambda+3}{2}+\mu}\int_0^\infty V(r)e^{-\frac{\nu r^2}{2}}r^{\lambda+2\mu+2}dr. \quad \text{(A7)}$$

In Table VIII we show the neutrino potentials in Tomoda's formulation [9] of $\beta\beta$ decay. In this table $\tilde{A} = \langle E_N \rangle - (E_I + E_F)/2$ is the closure energy, where $\langle E_N \rangle$ is the averaged energy of the intermediate nucleus and $E_{I,F}$ are the energies of the initial and final states. If $\tilde{A} = 0$, the potential $H(r)$ that appears in 0ν Fermi and Gamow-Teller transitions becomes the Coulomb potential $1/r$ with Fourier-Bessel transform $\frac{2}{\pi}\frac{1}{p^2}$. Table IX shows the neutrino potentials corresponding to the HOC terms in the Šimkovic formulation [10]. These potentials replace $v_0(p)$ for Fermi and Gamow-Teller transitions and $v_2(p)$ for tensor transitions in the radial integrals.

The radial integrals depend on the values of the oscillator parameter ν and the closure energy $\tilde{A}$. In this article we take $\nu = \nu_0 A^{-1/3}$, where A is the mass number and $\nu_0 = 0.994$ fm^{-2}. The values of $\tilde{A}$ are taken from Tomoda and are listed in Table X.

APPENDIX B: PAIR STRUCTURE CONSTANTS

In the definition of the pair operators Eqs. (7) and (8) there appear the pair structure constants α_j and $\beta_{jj'}$. In the 1980s, several theories were put forward to evaluate the structure constants [16]. In this article we use the simple prescription of Ref. [12] that is to obtain the coefficients by diagonalizing the

TABLE IX. Neutrino potentials corresponding to the HOC terms in the Šimkovic formulation adapted to our approach. The factor 3 for the tensor contributions is introduced to use them according to our definition of the tensor operator $S_{nn'}$. m_p and m_π are the proton and pion mass and $\kappa_\beta = 3.70$ is the isovector anomalous magnetic moment of the nucleon.

HOC term	$v_\lambda(p)$
h^F_{VV}	$\frac{2}{\pi}\frac{1}{p(p+\tilde{A})}\frac{g_V^2}{(1+p^2/M_V^2)^4}$
h^{GT}_{AA}	$\frac{2}{\pi}\frac{1}{p(p+\tilde{A})}\frac{1}{(1+p^2/M_A^2)^4}$
h^{GT}_{AP}	$\frac{2}{\pi}\frac{1}{p(p+\tilde{A})}[-\frac{2}{3}\frac{1}{(1+p^2/M_A^2)^4}\frac{p^2}{p^2+m_\pi^2}(1-\frac{m_\pi^2}{M_A^2})]$
h^{GT}_{PP}	$\frac{2}{\pi}\frac{1}{p(p+\tilde{A})}[\frac{1}{\sqrt{3}}\frac{1}{(1+p^2/M_A^2)^2}\frac{p^2}{p^2+m_\pi^2}(1-\frac{m_\pi^2}{M_A^2})]^2$
h^{GT}_{MM}	$\frac{2}{\pi}\frac{1}{p(p+\tilde{A})}[\frac{2}{3}\frac{g_V^2}{g_A^2}\frac{1}{(1+p^2/M_V^2)^4}\frac{\kappa_\beta^2 p^2}{4m_p^2}]$
h^T_{AP}	$-3h^{GT}_{AP}$
h^T_{PP}	$-3h^{GT}_{PP}$
h^T_{MM}	$\frac{3}{2}h^{GT}_{MM}$

SDI whose two-body matrix elements are given by

$$\begin{aligned}\langle j_a j_b|V|j_c j_d\rangle_{JT} &= (-1)^{n_a+n_b+n_c+n_d} A_T \\ &\times \sqrt{\frac{(2j_a+1)(2j_b+1)(2j_c+1)(2j_d+1)}{4(2J+1)^2(1+\delta_{ab})(1+\delta_{cd})}} \\ &\times \left\{(-1)^{j_b+l_b+j_d+l_d}\left\langle j_b -\frac{1}{2} j_a \frac{1}{2}\middle| J0\right\rangle\right. \\ &\times \left\langle j_d -\frac{1}{2} j_c \frac{1}{2}\middle| J0\right\rangle [1-(-1)^{l_a+l_b+J+T}] \\ &\left. -\left\langle j_b \frac{1}{2} j_a \frac{1}{2}\middle| J1\right\rangle\left\langle j_d \frac{1}{2} j_c \frac{1}{2}\middle| J1\right\rangle [1-(-1)^T]\right\}, \quad \text{(B1)}\end{aligned}$$

with A_T ($T = 1$, isovector; $T = 0$, isoscalar) the strength parameter, and by taking the lowest 0^+ and 2^+ states of identical nucleons as the collective S and D states. (For generating the coefficients α_j, $\beta_{jj'}$ in IBM-2 we need only the strength A_1.) The inputs in this calculation are the energies of the single particle orbitals and the strength parameters. To test the sensitivity of the calculation to the choice of the single-particle energies we have used two sets of single-particle energies: an "experimental" (Set I), obtained from the observed one-particle states; and a "theoretical" (Set II) as given in Ref. [26]. The corresponding single-particle energies are tabulated in Tables XI–XIII. A complication arises because the nuclei we calculate are in a wide range of mass numbers and cover several major shells. Also, in some cases, the protons are particles and the neutron are holes and vice-versa. The tables contain therefore both particle and hole energies as in Ref. [12]. The strength of the surface delta interaction is chosen to fit the $2^+ - 0^+$ energy difference in nuclei with either two protons (proton holes) or two neutrons (neutron holes) and is given in the same Tables XI–XIII.

From the single-particle energies and values of A_1, we obtain the structure coefficients given in Tables XIV–XVI. The overall sign in these coefficients is not important, because it will disappear when the the matrix elements are squared. However, the relative sign is of importance, and we use the approximate relation [12]

$$\beta_{jj'} = \frac{\alpha_j + \alpha_{j'}}{\sqrt{5}\Omega(1+\delta_{jj'})}\langle j\|r^2 Y_2\|j'\rangle \quad \text{(B2)}$$

to determine the sign of β relative to α. From Eq. (B2) we see that the relative sign of α versus β changes when going from particles to holes, because

$$\langle j^{-1}\|r^2 Y_2\|j'^{-1}\rangle = -\langle j\|r^2 Y_2\|j'\rangle. \quad \text{(B3)}$$

TABLE X. Closure energies $\tilde{A}$ used in this work. From Ref. [9].

	$\tilde{A}$ (MeV)
^{76}Ge → ^{76}Se	9.41
^{82}Se → ^{82}Kr	10.08
^{100}Mo → ^{100}Ru	11.2
^{128}Te → ^{128}Xe	12.54
^{130}Te → ^{130}Xe	13.28
^{136}Xe → ^{136}Ba	13.1
^{150}Nd → ^{150}Sm	13.7
^{154}Sm → ^{154}Gd	13.9

TABLE XI. SDI strength values A_1 and single-particle and hole energies (in MeV) in the $N, Z = 28$–50 shell. The energies are taken from the spectra of ^{57}Cu for proton particles, from isotones $N = 50$ for proton holes, from the spectra of ^{57}Ni for neutron holes (Set I), and from Fig. 2-30 in Ref. [26] for neutron holes (Set II).

Orbital	Protons (particles)	Protons (holes)	Neutrons (I) (holes)	Neutrons (II) (holes)
	$A_1 = 0.366$	$A_1 = 0.264$	$A_1 = 0.280$	$A_1 = 0.302$
$2p_{1/2}$	1.106	0.931	1.896	2.620
$2p_{3/2}$	0.000	2.198	3.009	4.470
$1f_{5/2}$	1.028	2.684	2.240	3.700
$1g_{9/2}$	3.009	0.000	0.000	0.000

TABLE XII. SDI strength values A_1 and single-particle and hole energies (in MeV) in the $N, Z = 50$–82 shell. The energies are taken from the spectra of ^{133}Sb for protons, from the spectra of ^{91}Zr for neutron particles (Set I), from the spectra of ^{131}Sn for neutron holes (Set I), and from Fig. 2-30 in Ref. [26] for neutron particles and holes (Set II).

Orbital	Protons (particles)	Neutrons (I) (particles)	Neutrons (II) (particles)	Neutrons (I) (holes)	Neutrons (II) (holes)
	$A_1 = 0.221$	$A_1 = 0.269$	$A_1 = 0.284$	$A_1 = 0.163$	$A_1 = 0.179$
$3s_{1/2}$	2.990	1.205	1.850	0.332	1.079
$2d_{3/2}$	2.690	2.042	2.543	0.000	0.848
$2d_{5/2}$	0.960	0.000	0.000	1.655	3.006
$1g_{7/2}$	0.000	2.200	1.387	2.434	2.775
$1h_{11/2}$	2.760	2.170	3.776	0.070	0.000

TABLE XIII. SDI strength values A_1 and single-particle energies (in MeV) in the $N = 82$–126 shell. The energies are taken from Ref. [12] for Set I and Fig. 2-30 in Ref. [26] for Set II.

Orbital	Neutrons (I) (particles)	Neutrons (II) (particles)
	$A_1 = 0.147$	$A_1 = 0.132$
$3p_{1/2}$	2.250	2.927
$3p_{3/2}$	1.500	1.927
$2f_{5/2}$	2.600	2.927
$2f_{7/2}$	0.000	0.000
$1h_{9/2}$	2.450	1.002
$1i_{13/2}$	2.800	2.927

APPENDIX C: GENERALIZED SENIORITY MATRIX ELEMENTS

In this appendix, we quote some matrix elements between SM states belonging to the SD subspace. These matrix elements are needed to calculate matrix elements of the double-β decay transition operator in the generalized seniority scheme. A general method for calculating *exactly* matrix elements in the generalized seniority scheme is the commutator method introduced by Frank and van Isacker [13] and by Lipas *et al.* [14]. We have used this method to evaluate the matrix elements of the pair operators $(\tilde{c}_j \times \tilde{c}_j)^{(0)}$ and $(\tilde{c}_j \times \tilde{c}_{j'})^{(2)}$ between states in the SD subspace. Labeling the states as $|n, v, J\rangle$, we obtain the following matrix elements

$$\begin{aligned}
&\langle n,0,0\|(\tilde{c}_j \times \tilde{c}_j)^{(0)}\|n+2,0,0\rangle \\
&= -\frac{\left(\frac{n}{2}+1\right)\left(\frac{n}{2}!\right)^2}{\eta_{n,0,0}\eta_{n+2,0,0}}\hat{\jmath}\alpha_j \sum_{s=0}^{n/2}(-1)^s\left(\frac{\alpha_j^s \eta_{n-2s,0,0}}{(\frac{n}{2}-s)!}\right)^2, \qquad \text{(C1)}\\
&\langle n,0,0\|(\tilde{c}_j \times \tilde{c}_{j'})^{(2)}\|n+2,2,2\rangle \\
&= -\sqrt{5(1+\delta_{jj'})}\frac{\eta^2_{n+2,2,2}(jj')}{\eta_{n,0,0}\eta_{n+2,2,2}}\beta_{jj'}, \qquad \text{(C2)}\\
&\langle n,2,2\|(\tilde{c}_j \times \tilde{c}_{j'})^{(2)}\|n+2,0,0\rangle \\
&= \left(\frac{n}{2}\right)\left(\frac{n}{2}+1\right)\alpha_j\alpha_{j'}(-1)^{j-j'} \\
&\quad \times \sqrt{5(1+\delta_{jj'})}\frac{\eta^2_{n,2,2}(j'j)}{\eta_{n+2,0,0}\eta_{n,2,2}}\beta_{j'j}, \qquad \text{(C3)}\\
&\langle n,2,2\|(\tilde{c}_j \times \tilde{c}_{j'})^{(L)}\|n+2,2,2\rangle \\
&= (-1)^L\left(\frac{n}{2}\right)\left(\frac{n}{2}-1\right)\alpha_j\alpha_{j'}\frac{\eta_{n-2,2,2}}{\eta_{n+2,2,2}} \\
&\quad \langle n-2\,2\,2\|(\tilde{c}_j \times \tilde{c}_{j'})^{(L)}\|n\,2\,2\rangle \\
&\quad -\left(\frac{n}{2}\right)\frac{\eta_{n,2,2}}{\eta_{n+2,2,2}}(\alpha_j + (-1)^L\alpha_{j'}) \\
&\quad \langle n\,2\,2\|(c_j^\dagger \times \tilde{c}_{j'})^{(L)}\|n\,2\,2\rangle \\
&\quad -\left(\frac{n}{2}\right)\frac{\eta_{n,2,2}}{\eta_{n+2,2,2}}\hat{\jmath}\alpha_j\delta_{jj'}\delta_{L0}\sqrt{5}, \qquad \text{(C4)}
\end{aligned}$$

TABLE XIV. Pair structure coefficients α_j and $\beta_{jj'}$ in the $N, Z = 28$–50 shell.

	Protons (particles)	Protons (holes)	Neutrons (I) (holes)	Neutrons (II) (holes)
$\alpha_{1/2}$	−0.850	0.689	0.468	0.382
$\alpha_{3/2}$	−1.867	0.408	0.336	0.251
$\alpha_{5/2}$	−0.884	0.352	0.418	0.293
$\alpha_{9/2}$	0.439	−1.401	−1.416	−1.447
$\beta_{1/2\,3/2}$	−0.322	−0.092	−0.063	−0.046
$\beta_{3/2\,3/2}$	−0.866	−0.048	−0.037	−0.026
$\beta_{1/2\,5/2}$	−0.234	−0.099	−0.091	−0.062
$\beta_{3/2\,5/2}$	0.222	0.040	0.039	0.026
$\beta_{5/2\,5/2}$	−0.182	−0.052	−0.064	−0.041
$\beta_{9/2\,9/2}$	0.093	0.988	0.990	0.996

TABLE XV. Pair structure coefficients α_j and $\beta_{jj'}$ in the $N, Z = 50$–82 shell.

	Protons (particles)	Neutrons (I) (particles)	Neutrons (II) (particles)	Neutrons (I) (holes)	Neutrons (II) (holes)
$\alpha_{1/2}$	0.382	0.852	0.667	−0.999	−0.644
$\alpha_{3/2}$	0.414	0.614	0.535	−1.395	−0.734
$\alpha_{5/2}$	0.817	1.921	1.957	−0.469	−0.318
$\alpha_{7/2}$	1.769	0.584	0.799	−0.357	−0.338
$\alpha_{11/2}$	−0.406	−0.589	−0.395	1.287	1.514
$\beta_{1/2\,3/2}$	−0.054	−0.118	−0.090	−0.402	−0.118
$\beta_{3/2\,3/2}$	0.040	0.068	0.056	0.492	0.093
$\beta_{1/2\,5/2}$	0.092	0.324	0.234	0.159	0.075
$\beta_{3/2\,5/2}$	0.053	0.115	0.096	0.098	0.042
$\beta_{5/2\,5/2}$	0.131	0.899	0.925	0.078	0.040
$\beta_{3/2\,7/2}$	0.170	0.149	0.160	0.176	0.109
$\beta_{5/2\,7/2}$	−0.131	−0.088	−0.128	−0.037	−0.024
$\beta_{7/2\,7/2}$	0.957	0.098	0.148	0.065	0.050
$\beta_{11/2\,11/2}$	−0.075	−0.124	−0.074	−0.721	−0.976

TABLE XVI. Pair structure coefficients α_j and $\beta_{jj'}$ in the $N = 82$–126 shell.

	Neutrons (I) (particles)	Neutrons (II) (particles)
$\alpha_{1/2}$	−0.418	−0.315
$\alpha_{3/2}$	−0.572	−0.445
$\alpha_{5/2}$	−0.371	−0.315
$\alpha_{7/2}$	−2.188	−2.119
$\alpha_{9/2}$	−0.390	−0.716
$\alpha_{13/2}$	0.349	0.315
$\beta_{1/2\,3/2}$	−0.057	−0.039
$\beta_{3/2\,3/2}$	−0.050	−0.035
$\beta_{1/2\,5/2}$	−0.055	−0.040
$\beta_{3/2\,5/2}$	0.034	0.026
$\beta_{5/2\,5/2}$	−0.039	−0.030
$\beta_{3/2\,7/2}$	−0.209	−0.148
$\beta_{5/2\,7/2}$	−0.043	−0.034
$\beta_{7/2\,7/2}$	−0.964	−0.971
$\beta_{5/2\,9/2}$	−0.082	−0.091
$\beta_{7/2\,9/2}$	0.039	0.076
$\beta_{9/2\,9/2}$	−0.055	−0.110
$\beta_{13/2\,13/2}$	0.058	0.048

TABLE XVII. Coefficients $A_\rho(j)$, $B_\rho(j,j')$, $C_\rho(j,j')$, and $D_\rho(j,j')$ for $N \geqslant 0$, where N is the number of pairs (bosons in the IBM) of protons ($\rho = \pi$) or neutrons ($\rho = \nu$). The letters p and h indicate particle or hole character.

π	ν	Restrictions	$A_\rho(j)$
p	h	$N \geqslant 0$	$\frac{\langle S^{N+1}\|(c_j^\dagger \times c_{j'}^\dagger)^{(0)}\|S^N\rangle}{\langle s^{N+1}\|s^\dagger\|s^N\rangle} = -\frac{\langle 2N\,0\,0\|(\tilde{c}_j \times \tilde{c}_{j'})^{(0)}\|2N+2\,0\,0\rangle}{\sqrt{N+1}}$
h	p	$N \geqslant 1$	$\frac{\langle S^{N-1}\|(\tilde{c}_j \times \tilde{c}_{j'})^{(0)}\|S^N\rangle}{\langle s^{N-1}\|\tilde{s}\|s^N\rangle} = \frac{\langle 2N-2\,0\,0\|(\tilde{c}_j \times \tilde{c}_{j'})^{(0)}\|2N\,0\,0\rangle}{\sqrt{N}}$
π	ν	Restrictions	$B_\rho(j,j')$
p	h	$N \geqslant 0$	$\frac{\langle DS^N\|(c_j^\dagger \times c_{j'}^\dagger)^{(2)}\|S^N\rangle}{\langle ds^N\|d^\dagger\|s^N\rangle} = (-1)^{j+j'}\frac{\langle 2N\,0\,0\|(\tilde{c}_{j'} \times \tilde{c}_j)^{(2)}\|2N+2\,2\,2\rangle}{\sqrt{5}}$
h	p	$N \geqslant 1$	$\frac{\langle S^{N-1}\|(\tilde{c}_j \times \tilde{c}_{j'})^{(2)}\|DS^{N-1}\rangle}{\langle s^{N-1}\|\tilde{d}\|ds^{N-1}\rangle} = \frac{\langle 2N-2\,0\,0\|(\tilde{c}_j \times \tilde{c}_{j'})^{(2)}\|2N\,2\,2\rangle}{\sqrt{5}}$
π	ν	Restrictions	$C_\rho(j,j')$
p	h	$N \geqslant 1$	$\frac{\langle S^{N+1}\|(c_j^\dagger \times c_{j'}^\dagger)^{(2)}\|DS^{N-1}\rangle}{\langle s^{N+1}\|s^\dagger\tilde{s}^\dagger\tilde{d}\|ds^{N-1}\rangle} = (-1)^{j+j'}\frac{\langle 2N\,2\,2\|(\tilde{c}_{j'} \times \tilde{c}_j)^{(2)}\|2N+2\,0\,0\rangle}{\sqrt{5N(N+1)}}$
h	p	$N \geqslant 2$	$\frac{\langle DS^{N-2}\|(\tilde{c}_j \times \tilde{c}_{j'})^{(2)}\|S^N\rangle}{\langle ds^{N-2}\|\tilde{s}\tilde{s}d^\dagger\|s^N\rangle} = \frac{\langle 2N-2\,2\,2\|(\tilde{c}_j \times \tilde{c}_{j'})^{(2)}\|2N\,0\,0\rangle}{\sqrt{5N(N-1)}}$
π	ν	Restrictions	$D_\rho(j,j')$
p	h	$N \geqslant 1$	$\frac{\langle DS^N\|(c_j^\dagger \times c_{j'}^\dagger)^{(2)}\|DS^{N-1}\rangle}{\langle ds^N\|s^\dagger(d^\dagger\tilde{d})^{(2)}\|ds^{N-1}\rangle} = (-1)^{j+j'}\frac{\langle 2N\,2\,2\|(\tilde{c}_{j'} \times \tilde{c}_j)^{(2)}\|2N+2\,2\,2\rangle}{\sqrt{5N}}$
h	p	$N \geqslant 2$	$\frac{\langle DS^{N-2}\|(\tilde{c}_j \times \tilde{c}_{j'})^{(2)}\|DS^{N-1}\rangle}{\langle ds^{N-2}\|\tilde{s}(d^\dagger\tilde{d})^{(2)}\|ds^{N-1}\rangle} = \frac{\langle 2N-2\,2\,2\|(\tilde{c}_j \times \tilde{c}_{j'})^{(2)}\|2N\,2\,2\rangle}{\sqrt{5(N-1)}}$

where

$$\eta^2_{n,0,0} = \left(\frac{n}{2}!\right)^2 \sum_{\substack{m_1 \ldots m_k \\ \sum_i m_i = n/2}} \left\{ \prod_{i=1}^{k} \alpha_{j_i}^{2m_i} \binom{\Omega_{j_i}}{m_i} \right\}, \tag{C5}$$

$$\eta^2_{n,2,2} = \sum_{j \leqslant j'} \beta^2_{jj'} \eta^2_{n,2,2}(jj'), \tag{C6}$$

$$\eta^2_{n,2,2}(jj') = \sum_{p=0}^{\frac{n}{2}-1} \left[\frac{\left(\frac{n}{2}-1\right)!}{p!}\right]^2 (-1)^{\frac{n}{2}-1-p} \eta^2_{2p,0,0} \times \sum_{q=0}^{\frac{n}{2}-1-p} \alpha_j^{n-2-2p-2q} \alpha_{j'}^{2q} \tag{C7}$$

$$\langle n,2,2\|(c_j^\dagger \times \tilde{c}_{j'})^{(L)}\|n,2,2\rangle = -5\hat{L} \sum_i \beta_{ij}\beta_{j'i}\sqrt{(1+\delta_{ij})(1+\delta_{ij'})} \begin{Bmatrix} j & L & j' \\ 2 & i & 2 \end{Bmatrix} \times \frac{\alpha_j \alpha_{j'} \left(\frac{n}{2}-1\right)^2 \eta^2_{n-2,2,2}(ij) - (-1)^L \eta^2_{n,2,2}(ij)}{\eta^2_{n,2,2}} - \frac{\eta^2_{n-2,2,2}}{\eta^2_{n,2,2}} \left(\frac{n}{2}-1\right)^2 \alpha^2_{j'} [\sqrt{5}\hat{j}\delta_{jj'}\delta_{L0} + \langle n-2\,2\,2\|(c_j^\dagger \times \tilde{c}_{j'})^{(L)}\|n-2\,2\,2\rangle]. \tag{C8}$$

The recurrence relations (C4) and (C8) are of the form

$$f(n) = a_n f(n-2) + b_n, \tag{C9}$$

which can be solved to give the general expression

$$f(n) = \sum_{p=1}^{\frac{n}{2}} \left(\prod_{k=p+1}^{\frac{n}{2}} a_{2k} \right) b_{2p}, \tag{C10}$$

because in both cases $f(0) = 0$ and $f(2) = b_2$.

We have checked these expressions for the case of a single-j shell, in which $\alpha_j = \beta_{jj} = 1$, and

$$\eta^2_{n,0,0} = \left[\left(\frac{n}{2}\right)!\right]^2 \binom{\Omega_j}{n/2}, \tag{C11}$$

$$\eta^2_{n,2,2} = \eta^2_{n\,2\,2}(jj) = \left[\left(\frac{n}{2}-1\right)!\right]^2 \binom{\Omega_j - 2}{n/2-1}, \tag{C12}$$

and obtained

$$\langle n,0,0\|(\tilde{c}_j \times \tilde{c}_j)^{(0)}\|n+2,0,0\rangle = -\sqrt{\frac{(n+2)(2\Omega_j - n)}{2\Omega_j}}, \tag{C13}$$

$$\langle n,0,0\|(\tilde{c}_j \times \tilde{c}_j)^{(2)}\|n+2,2,2\rangle = -\sqrt{\frac{5(2\Omega_j - n - 2)(2\Omega_j - n)}{2\Omega_j(\Omega_j - 1)}}, \tag{C14}$$

TABLE XVIII. Hamiltonian parameters employed in the IBM-2 calculations of the initial and final wave functions along with their references.

Nucleus	Ref.	ϵ_{d_ν}	ϵ_{d_π}	κ	χ_ν	χ_π	ξ_1	ξ_2	ξ_3	$c_\nu^{(0)}$	$c_\nu^{(2)}$	$c_\nu^{(4)}$	$c_\pi^{(0)}$	$c_\pi^{(2)}$
^{76}Ge	[27]	1.20	1.20	−0.21	1.000	−1.200	−0.05	0.10	−0.05					
^{76}Se	[28]	0.96	0.96	−0.16	0.500	−0.900			−0.10					
^{82}Se	[28]	1.00	1.00	−0.28	1.140	−0.900			−0.10					
^{82}Kr	[29]	1.15	1.15	−0.19	0.925	−1.127	−0.10		−0.10					
^{100}Mo	[30]	0.55	1.00	−0.06	−1.200	0.400	−0.10	0.10	−0.10	−0.6	0.20	0.100		
^{100}Ru	[31]	0.89	0.89	−0.18	−1.000	0.400				0.6	0.09	−0.125		
^{128}Te	[32]	0.93	0.93	−0.17	0.500	−1.200	−0.18	0.24	−0.18	0.3	0.22			
^{128}Xe	[32]	0.70	0.70	−0.17	0.330	−0.800	−0.18	0.24	−0.18	0.3				
^{130}Te	[32]	1.05	1.05	−0.20	0.900	−1.200	−0.18	0.24	−0.18	0.3	0.22			
^{130}Xe	[32]	0.76	0.76	−0.19	0.500	−0.800	−0.18	0.24	−0.18	0.3	0.22			
^{150}Nd	[33]	0.47	0.47	−0.07	−1.000	−1.200	−0.12	0.24	0.90				0.4	0.20
^{150}Sm	[33]	0.70	0.70	−0.08	−0.800	−1.300	−0.12	0.24	0.90					0.05
^{154}Sm	[33]	0.43	0.43	−0.081	−1.100	−1.300	−0.12	0.24	0.90					0.05
^{154}Gd	[33]	0.55	0.55	−0.080	−1.000	−1.000	−0.12	0.24	0.90				−0.2	−0.1

$$\langle n,2,2\|(\tilde{c}_j\times\tilde{c}_j)^{(2)}\|n+2,0,0\rangle = \sqrt{\frac{5n(n+2)}{2\Omega_j(\Omega_j-1)}}, \tag{C15}$$

$$\langle n,2,2\|(\tilde{c}_j\times\tilde{c}_j)^{(2)}\|n+2,2,2\rangle = -\frac{10(\Omega_j+2)}{\sqrt{7j(j+1)}}\sqrt{\frac{n(2\Omega_j-n-2)}{\Omega_j(\Omega_j-1)(\Omega_j+1)}}, \tag{C16}$$

$$\langle n,2,2\|(c_j^\dagger\times\tilde{c}_j)^{(2)}\|n,2,2\rangle = \frac{10}{\sqrt{7j(j+1)}}\frac{(\Omega_j-n)(\Omega_j+2)}{\sqrt{\Omega_j(\Omega_j-1)(\Omega_j+1)}}, \tag{C17}$$

which coincide with the expressions which can be deduced from [16].

APPENDIX D: COEFFICIENTS OF THE BOSON MAPPING

We give in Table XVII the coefficients $A_\rho(j)$, $B_\rho(j,j')$, $C_\rho(j,j')$, $D_\rho(j,j')$ of the boson mapping ($\rho=\pi,\nu$) in terms of the generalized seniority matrix elements of the type

$$\langle n,v,J\|(\tilde{c}_j\times\tilde{c}_{j'})^{(I)}\|n+2,v',J'\rangle, \tag{D1}$$

where n is the total number of identical nucleons, v and v' are the generalized seniorities, and J and J' the total angular momenta of the final and initial states, respectively. N in this table is the number of pairs (bosons) in the IBM.

APPENDIX E: PARAMETERS OF THE IBM-2 HAMILTONIAN

To obtain matrix elements of the transition operators in double β decay we use *realistic* IBM-2 wave functions taken from the literature that have been shown to provide an accurate description of many properties (energies, electromagnetic transition rates, quadrupole and magnetic moments, etc.) of the final and initial nuclei. A detailed description of the IBM-2 Hamiltonian is given in Refs. [17,34]. The values of the Hamiltonian parameters, as well as the references from which they were taken, are given in Table XVIII.

[1] Y. Fukuda *et al.*, Phys. Rev. Lett. **81**, 1562 (1998).
[2] Q. R. Ahmad *et al.*, Phys. Rev. Lett. **89**, 011301 (2002).
[3] K. Eguchi *et al.*, Phys. Rev. Lett. **90**, 021802 (2003).
[4] H. V. Klapdor-Kleingrothaus *et al.*, Phys. Lett. **B586**, 198 (2004).
[5] E. Fiorini, in *Proc. Int. School "Enrico Fermi," Course CLXIX*, edited by A. Covello *et al.* (IOS Press, Amsterdam, 2008), p. 477.
[6] R. Arnold *et al.*, Phys. Rev. Lett. **95**, 182302 (2005).
[7] W. C. Haxton and G. J. Stephenson, Jr., Prog. Part. Nucl. Phys. **12**, 409 (1984).
[8] E. Caurier, J. Menéndez, F. Nowacki, and A. Poves, Phys. Rev. Lett. **100**, 052503 (2008).
[9] T. Tomoda, Rep. Prog. Phys. **54**, 53 (1991).
[10] F. Šimkovic, G. Pantis, J. D. Vergados, and A. Faessler, Phys. Rev. C **60**, 055502 (1999).
[11] A. de-Shalit and I. Talmi, *Nuclear Shell Theory* (Academic Press, New York, 1963).
[12] S. Pittel, P. D. Duval, and B. R. Barrett, Ann. Phys. (N.Y.) **144**, 168 (1982).
[13] A. Frank and P. Van Isacker, Phys. Rev. C **26**, 1661 (1982).
[14] P. O. Lipas, M. Koskinen, H. Harter, R. Nojarov, and A. Faessler, Nucl. Phys. **A508**, 509 (1990).
[15] A. Arima, T. Otsuka, F. Iachello, and I. Talmi, Phys. Lett. **B66**, 205 (1977).
[16] T. Otsuka, A. Arima, and F. Iachello, Nucl. Phys. **A309**, 1 (1978).
[17] F. Iachello and A. Arima, *The Interacting Boson Model* (Cambridge University Press, Cambridge, 1987).
[18] O. Scholten and Z. R. Yu, Phys. Lett. **B161**, 13 (1985).
[19] J. Menéndez, A. Poves, E. Caurier, and F. Nowacki, Nucl. Phys. **A818**, 139 (2008).

[20] F. Šimkovic, A Faessler, V. Rodin, P. Vogel, and J. Engel, Phys. Rev. C **77**, 045503 (2008).
[21] J. P. Schiffer *et al.*, Phys. Rev. Lett. **100**, 112501 (2008).
[22] J. Suhonen and O. Civitarese, Phys. Lett. B **668**, 277 (2008).
[23] A. Arima and F. Iachello, Phys. Rev. C **16**, 2085 (1977).
[24] J. N. Bahcall, H. Murayama, and C. Pe̋na-Garay, Phys. Rev. D **70**, 033012 (2004).
[25] H. Horie and K. Sasaki, Prog. Theor. Phys. **25**, 475 (1961).
[26] A. Bohr and B. R. Mottelson, *Nuclear Structure* (W. A. Benjamin Inc, New York, 1969), Vol. I.
[27] P. D. Duval, D. Goutte, and M. Vergnes, Phys. Lett. **B124**, 297 (1983).
[28] U. Kaup, C. Mnkemeyer, and P. V. Brentano, Z. Phys. A **310**, 129 (1983).
[29] U. Kaup and A. Gelberg, Z. Phys. A **293**, 311 (1979).
[30] H. Dejbakhsh, D. Latypov, G. Ajupova, and S. Shlomo, Phys. Rev. C **46**, 2326 (1992).
[31] P. Van Isacker and G. Puddu, Nucl. Phys. **A348**, 125 (1980).
[32] G. Puddu, O. Scholten, and T. Otsuka, Nucl. Phys. **A348**, 109 (1980).
[33] O. Scholten, Ph. D. thesis, University of Groningen, The Netherlands, 1980.
[34] T. Otsuka and N. Yoshida, user's manual of the program NPBOS, Report No. JAERI-M 85-094, 1985.